https://doi.org/10.5194/egusphere-2025-5969
Preprint. Discussion started: 18 December 2025

CO_2 and H_2O isotope exchange and flux partitioning in Amazonia

Robbert P.J. Moonen[a], Getachew A. Adnew[b], Jordi Vilà-Guerau de Arellano[c], David J. Bonell Fontas[a], and Thomas Röckmann[a]

[a]Institute for Marine and Atmospheric Research, Utrecht University, Heidelberglaan 8, 3584CS, The Netherlands
[b]Department of Geosciences and Natural Resource Management, University of Copenhagen, Øster Voldgade 10, 1350 Copenhagen K, Denmark
[c]Meteorology and Air Quality Group, Wageningen University, Droevendaalsesteeg 4, 6708PB, The Netherlands

Correspondence: Robbert P.J. Moonen (robbert_moonen@live.nl)

Abstract. Understanding the coupled exchange of H_2O and CO_2 between ecosystems and the atmosphere remains limited due to our inability to partition net fluxes into their individual source and sink components. For the Amazon rainforest, which plays an important role in the global balance of water and carbon, investigating these individual fluxes is critical given the environmental changes in recent years. Here, we apply a stable isotope-based approach to partition ecosystem-scale gas exchange from simultaneous eddy covariance measurements of H_2O and CO_2 isotopologues. During the 2022 CloudRoots-Amazon campaign at the Amazon Tall Tower Observatory, high-frequency isotope flux measurements from 57 m were used to derive multi-day composite diurnal cycles of δ fluxes and ecosystem source compositions. A steady-state midday interval, constrained with independent leaf and soil isotopic observations, allowed us to coherently link the H_2O and CO_2 isotopic states throughout the ecosystem (soil, canopy, leaf, atmosphere) using $\delta^{18}O$.

Isotopic flux partitioning indicates that transpiration accounts for 95.5 $\%$ of the net evapotranspiration (ET) of water at 14:00, with soil evaporation being responsible for 4.5 $\%$. For CO_2, $\delta^{18}O$-based partitioning indicates that the respiration flux from the soil equals -44 $\%$ of the net ecosystem exchange (NEE), where the photosynthetic assimilation flux in turn is 144 $\%$ of NEE. The partitioning of NEE was found to be strongly dependent on the leaf intercellular-to-atmospheric CO_2 ratio (c_i/c_a) which determines the (apparent) isotopic composition associated with photosynthetic assimilation (δ_P). This underlines how important detailed leaf and soil level measurements of isotopic compositions and leaf characteristics are for ecosystem-scale flux partitioning.

1 Introduction

Tropical rainforests are key drivers of the global water and carbon cycles (Bastos et al., 2020; Dominguez et al., 2022). However, the dynamics of these ecosystems are changing as a result of deforestation and climate change (Artaxo, 2023; Espinoza et al., 2024). The Amazon rainforest, which is world's largest, is changing from a net carbon sink to a source (Brienen et al., 2015; Ke et al., 2024). Unprecedented droughts and forest fires in recent years are signals of that change (Moreira et al., 2024; Mataveli et al., 2024).

https://doi.org/10.5194/egusphere-2025-5969
Preprint. Discussion started: 18 December 2025

Ecosystem scale measurements of the gas exchange of H_2O and CO_2 enable us to understand ecosystem dynamics (Baldocchi, 2014). However, common approaches for measuring the exchange are only able to assess the net exchange, which is the sum of several individual processes. The net ecosystem exchange of carbon dioxide (NEE) is the sum of the uptake by photosynthesis (P) and the release by respiration (R). Here, R is the sum of photo-respiration, dark respiration, and heterotrophic respiration. For water vapour, the main components of the net Evapotranspiration (ET) flux are the transpiration from vegetation (T), and evaporation (E) from soils. Note that after precipitation or during dewfall, a separate evaporation flux from intercepted water might be defined (Wei et al., 2017).

The inability to measure individual ecosystem fluxes separately is an important limitation in advancing our understanding of ecosystem dynamics. This is because environmental drivers are linked to individual gross fluxes, and relate only indirectly to net fluxes (Tramontana et al., 2020; Stoy et al., 2019). These process-based individual fluxes can be implemented in mathematical models to understand the relative importance and possible changes in individual exchange processes. Soil and leaf scale measurements provide accurate individual fluxes at small scales, but connecting those to the canopy and ecosystem scale is challenging (Sabot et al., 2022; González-Armas et al., 2024; Mangan et al., 2023). Stable isotopes can serve as natural tracers to address this limitation.

The isotopic composition is generally expressed in δ-notation, which is defined as :

$$\delta = \frac{R_{spl}}{R_{ref}} - 1 \tag{1}$$

Where R_{spl} indicates the heavy-to-light isotope ratio of the sampled compound, and R_{ref} represents the same isotope ratio of a common reference material (Mook and Geyh, 2000). In this work, we focus on the D isotope in H_2O, and the ^{18}O isotope in both H_2O and CO_2, for which Vienna Standard Mean Ocean Water (VSMOW) is the common reference ($^{D}R_{ref}$ = 0.00015575 and $^{18}R_{ref}$ = 0.0020052).

In natural ecosystems, small differences (‰) occur between the rate of exchange of various isotopologues dependent on the process. These differences can be used to attribute changes in isotopic compositions to specific environmental exchange processes, such as transpiration. For the application of ecosystem flux partitioning, flux measurements of the isotopic composition in the atmosphere δ_{atm} must be made in combination with measurements of the isotopic compositions of the relevant exchange reservoirs, e.g., soil water, leaf water or soil carbon isotopic composition (Barbour et al., 2017; Wehr and Saleska, 2015). In Sec. 2 we define the δ fluxes and describe how the ecosystem end-member compositions are quantified making use of collocated measurements of environmental variables and isotopic compositions.

Isotopic flux partitioning can be applied to all relevant isotopologues, potentially offering multiple, complementary handles. For example, water fluxes can be constrained independently using both ^{18}O and D isotopes. ^{18}O provides an interesting cross-species link because ^{18}O exchanges rapidly between H_2O and CO_2 in leaves, catalysed by the enzyme Carbonic Anhydrase (CA). For this reason, ^{18}O has shown to be a valuable link between the carbon and water cycles (Gillon and Yakir, 2001).

In this work, we for the first time investigate the connected carbon and water cycles by making use of comprehensive measurements of H_2O and CO_2 isotopic fluxes, vertical profiles of the state variables and discrete air, leaf and soil water

https://doi.org/10.5194/egusphere-2025-5969
Preprint. Discussion started: 18 December 2025

isotopic samples, and leaf gas exchange measurements. We base our analysis on the CloudRoots-Amazon22 dataset, which was acquired at the Amazon Tall Tower Observatory (ATTO) site in Brazil (see Sec. 3). We describe the diurnal cycles of the observed isotopic fluxes and discuss the isotopic state of the ecosystem. For a midday steady state period we then determine the end member isotopic compositions of individual gross fluxes. This allows us to systematically partition the net ecosystem fluxes into its individual components, which enables high resolution simulations of the water and the carbon cycles to be validated (Pedruzo-Bagazgoitia et al., 2023). In addition, our observations help to probe our biogeochemical understanding of the ^{18}O exchange at the ecosystem scale (Farquhar and Lloyd, 1993).

2 Theory

Stable isotope measurements of atmospheric species can be used to partition multiple sources and sinks of the same compound, which cannot be done with mole fraction information only (Wehr and Saleska, 2015; Oikawa et al., 2017). Mathematically, a system of two exchange equations is solved for two source fluxes. Given the land-atmosphere exchange of H_2O, it can be applied to partition evapotranspiration (ET) into evaporation (E) and transpiration (T). In this section, we first detail ET partitioning using the stable deuterium (D) isotope and subsequently show how the NEE of CO_2 can be partitioned into P and R using the ^{18}O isotope. Note that in the results, both the D and ^{18}O signatures of H_2O are used for ET partitioning. The following set of equations is specific to the example of ET partitioning using D, but can be used for NEE and ^{18}O as well (Bowling et al., 2001).

$$\begin{aligned} ET &= E + T \\ \delta D_{ET} * ET &= \delta D_E * E + \delta D_T * T \end{aligned} \tag{2}$$

Here, δD_{ET} is the deuterium isotopic composition of the net water vapour flux due to both evaporation and transpiration, δD_E is the isotopic composition of the evaporated water, and δD_T of the transpired water. This approach enables us to constrain a system with two individual gross fluxes contributing to the net flux. When more source terms are described, other isotopic or non-isotopic constraints can be added, or a-priori assumptions between the tracers need to be used. For the system represented in the above equations, none of the three isotope parameters (δD_{ET}, δD_E, and δD_T) are easily obtained and in the following section we describe the methods to acquire each of them.

The isotopic composition of the net exchange flux

The isotopic composition of the net exchange flux (δ_{ET} or δ_{NEE}) is comparable to the source isotopic composition being mixed into a reservoir. The difference is that δ_{ET} and δ_{NEE} can also describe the composition of a negative (uptake) flux. The common approach for determining the isotopic composition of a source from atmospheric measurements are mixing models, as described by Keeling (1958) and Miller and Tans (2003). In these models, changes in atmospheric isotopic compositions are directly related to changes in mole fractions. For example, when increased mole fractions are associated with enriched isotopic

https://doi.org/10.5194/egusphere-2025-5969
Preprint. Discussion started: 18 December 2025

compositions, the source is understood to be more enriched than the atmospheric background. In the Miller-Tans (MT) method, the slope of the relationship between $\delta\chi$ and χ is solved for to find the isotopic composition of the source (example in appendix Fig. A1). In various studies, the MT method has been used to determine δ_{ET} or δ_{NEE} irrespective of the flux sign (Griffis, 2013; Finkenbiner et al., 2022). We refer to estimates using the MT methods with $\delta_{...,MT}$.

The isotopic composition of the net turbulent exchange flux can also be estimated with measurements of the turbulent exchange fluxes of the various isotopologues of the target species (Griffis et al., 2007). δ fluxes (F_δ) provide a common method to determine such an isotope flux.

$$F_\delta = \overline{w'\delta'} \tag{3}$$

where, w' and δ' are the fluctuating components of the vertical wind and isotopic composition, respectively, after Reynolds decomposition (Bird, 2002). F_δ has the units $‰\,\mathrm{m\,s^{-1}}$. For the example of δD in water, $F_{\delta D}$ is related to the isotopic composition of the net flux (δD_{ET}), the atmospheric isotopic composition (δD_{atm}), and the total exchange flux (in this case ET) as follows (Lee et al., 2012).

$$F_{\delta D} = \frac{ET}{\rho_v^{atm}} * (\delta D_{ET,F} - \delta D_{atm}) \tag{4}$$

Here, ET is the evapotranspiration flux in $\mathrm{g\,m^{-2}\,s^{-1}}$. ρ_v^{atm} is the atmospheric absolute humidity in $\mathrm{g\,m^{-3}}$, and $\delta\mathrm{D}_{atm}$ is the atmospheric isotopic composition of deuterium in water vapour. Note that the fraction $\frac{ET}{\rho_v^{atm}}$ defines an exchange rate. The unit grams in the nominator and denominator can thus be replaced by moles. The isotopic composition of the net exchange flux (δD_{ET}), determined using this flux method ($\delta_{...,F}$), can be solved for and inserted into Eq. 2.

Until recently, the δ flux (F_δ) could only be inferred by relating gradient measurements of isotopologues to an exchange coefficient depending on mechanical and convective turbulence (Griffis et al., 2004; Yakir and da Silveira Lobo Sternberg, 2000). Now, high flow rate laser spectrometers are available which measure the isotopic composition at sub-second frequencies, which allow for direct isotope flux measurements using the eddy correlation technique. The difficultly in using such measurements is keeping the instrument stable, while maintaining high flow rates and an undisturbed inlet gas stream, which is necessary to resolve both the longest and shortest turbulent exchange timescales (Kolmogorov, 1941). We found that temperature-stabilized enclosures, combined with short, heated inlet lines provide a workable mode of adhering to these constraints (see Sec. 3).

2.1 The H_2O isotopic state

The isotopic composition of soil evaporation

Soil water samples can inform us of the isotopic composition of the soil evaporation $\delta\mathrm{D_E}$, which is required to solve eq 2. When calculating the isotopic composition of water evaporating from soils from the soil water isotopic composition, the temperature dependent isotopic fractionation of the liquid-to-gas phase change (evaporative fractionation) needs to be taken into account. The isotopic fractionation factor for deuterium ($\alpha_{\mathrm{l-v,D}}$) as determined by Horita and Wesolowski (1994) is:

https://doi.org/10.5194/egusphere-2025-5969
Preprint. Discussion started: 18 December 2025

$$10^3 ln(\alpha_{l-v,D}) = 1158.8(T^3/10^9) - 1620.1(T^2/10^6) + 794.84(T/10^3) - 161.04 + 2.9992(10^9/T^3) \quad (5)$$

Here, T is the temperature expressed in K, $\alpha_{\mathrm{l-v,D}}$ is the isotopic fractionation factor for deuterium when transitioning from a liquid ($_{\mathrm{l}}$) to a vapour ($_{\mathrm{v}}$) state.

For a given deuterium isotopic composition of liquid soil water, the isotopic fractionation factor can be used to calculate the equilibrium isotopic composition of the water vapour with (Mook and Geyh, 2000):

$$R_{D,v} = R_{D,ref}(\delta_{D,v} + 1) = \frac{R_{D,l}}{\alpha_{l-v,D}} \quad (6)$$

The main simplification in using the equilibrium water vapour isotopic composition to estimate δ_E is that kinetic fractionation effects taking place during diffusion into the atmosphere are not taken into account. Physically accurate representations of this kinetic fractionation are available, but complex. Kiemle et al. (2023) share a full complexity model, and find that using equilibrium fractionation only is a good first order approximation.

The isotopic composition of transpiration

Generally, the isotopic composition of δD_T is set equal to the isotopic composition of the source water in the soil ($\delta \mathrm{D_S}$), using the assumption of isotopic steady-state (Craig and Gordon, 1965). This is an expansion of the idea that when taking the leaf as a reservoir, the mass of the water entering the leaf matches the mass of the water evaporating from the leaf. No mass nor isotopic signal can be accumulated in leaves on longer timescales. On short timescales, the leaf water will act as a buffer when environmental conditions are changing (Dongmann et al., 1974).

The (δD_S) taken up by a plant represents the average of the water isotopic gradient in the root zone, weighted by the root water uptake at each depth (de Deurwaerder et al., 2020; Sutanto et al., 2014). This composition can be determined directly from a tree by sampling the water in the xylem. There is no fractionation associated with root water uptake, or transport through a tree (Rothfuss and Javaux, 2017).

The isotopic composition of water at evaporation sites

The average liquid water isotopic composition of leaves can be determined by collecting and analysing leaf samples. However, the isotopic composition of transpiration is related specifically to the water isotopic composition at the evaporation site in the stomata. The Craig-Gordon model, following Farquhar et al. (2007), accounts for the bidirectional isotopic exchange between atmospheric water vapour and the liquid water at the evaporation site.

$$R_e = \alpha_{l-v}[\alpha_k R_s(1 - \frac{w_a}{w_i}) + R_v \frac{w_a}{w_i}] \quad (7)$$

https://doi.org/10.5194/egusphere-2025-5969
Preprint. Discussion started: 18 December 2025

Here, $\mathrm{R_e}$ is the isotope ratio of liquid water at the evaporation site, $\mathrm{R_S}$ is the isotope ratio of the liquid source water, $\mathrm{R_v}$ is the isotope ratio of atmospheric water vapour, and $\mathrm{w_i}$ and $\mathrm{w_a}$ are the water vapour mole factions in the intercellular air space and in the atmosphere respectively.

The $\frac{\mathrm{w_a}}{\mathrm{w_i}}$ ratio can be interpreted as a relative humidity gradient and is used to describe the bidirectional diffusion of water vapour through stomata. Two terms in Eq. 7 contain the $\frac{\mathrm{w_a}}{\mathrm{w_i}}$ ratio, and together sum to 1. The $1-\frac{w_a}{w_i}$ term is associated to newly evaporated water, while the $\frac{w_a}{w_i}$ term is instead related to back-diffusion of ambient vapour. Together, both determine R_e, with $\frac{w_a}{w_i}$ indicating which process has a proportionally larger influence. At a certain leaf temperature, the internal concentration $\mathrm{w_i}$ is generally assumed to be equal to the temperature dependent saturation vapour pressure. While we make use of this assumption, we are aware that Cernusak et al. (2024) recently reported that this assumption is not always valid. The $\frac{\mathrm{w_a}}{\mathrm{w_i}}$ ratio is referred to with the symbol h in some literature (Farquhar and Cernusak, 2005).

α^{k} is the kinetic fractionation describing the faster diffusion for the light, abundant isotopologues. Farquhar et al. (1989a) quantified this fractionation step using the widely-applied resistance formulation, as shown in eq. 8.

$$\alpha_k(D) = 1 + \frac{0.025r_s + 0.017r_b}{r_s + r_b + r_a} \tag{8}$$

Here, r_s, r_b, and r_a are the stomatal, leaf boundary layer, and aerodynamic resistances respectively, in $\mathrm{sm^{-1}}$. The numbers 0.025 and 0.017 originate from 1.025 and 1.017, which are the kinetic fractionation factors for HDO compared to HHO for stomatal and boundary layer diffusion, respectively (Farquhar et al., 1989a). For ^{18}O, the kinetic fractionation factors are 1.032 for stomatal diffusion and 1.021 for the boundary layer diffusion (Lee et al., 2009). As transport to the atmosphere outside the leaf boundary layer is not a diffusive process, $\mathrm{r_a}$ does not cause kinetic fractionation.

The structure of Eq. 8 is the result of the transport pathway, where resistances associated to different physical transport processes (diffusion through stomata, diffusion though air in the leaf boundary layer, turbulent transport) are presented in series. Here, the largest resistance is the rate limiting step, and dominates the net fractionation effect. When the process is more diffusive, the related fractionation effect is larger. The theoretical kinetic fractionation factor for diffusion of HDO and HHO in free air, determined using the respective diffusivities (κ), is 1.0274. For diffusion through stomata or though the boundary layer this potential fractionation effect is reduced, as both processes are not purely diffusive. Boundary layer resistance is partially related to turbulent transport, which does not itself cause any fractionation (Lee et al., 2009). In contrast, transport through the stomata is near purely diffusive, resulting in larger fractionations factors, closer to the theoretical value. So far, empirical experiments have been used to quantify the fractionation factor specific to a context (Cappa et al., 2003).

The Péclet effect: Linking leaf samples to the evaporation site isotopic composition

A strong isotopic gradient can be present from the leaf veins to the evaporation site as a consequence of transpiration itself. This is because the light isotopologues evaporate preferentially from the liquid phase (Eq. 5), resulting in an enriched liquid water reservoir in the mesophyll. Back diffusion will act to diminish this gradient, but is limited during daytime due to the continual water flux from vein to the atmosphere, through the mesophyll (Cernusak et al., 2016).

https://doi.org/10.5194/egusphere-2025-5969
Preprint. Discussion started: 18 December 2025

The bidirectional scalar transport by advection and by diffusion results in a Péclet effect (Bird, 2002). Here, the dimensionless Péclet number (ϕ) indicates the relative magnitude of the advective flow compared to the diffusive relaxation, where positive numbers indicate advective dominance. In leaves, Péclet numbers are generally high during daytime, and low during nighttime, dependent on the transpiration flux T (Cernusak et al., 2016).

$$\phi = \frac{T\,L}{\rho_{lw}\,\kappa} \tag{9}$$

Here, T is the transpiration rate in $\mathrm{g\,m^{-2}\,s^{-1}}$, L is the length scale over which the Péclet effect takes place, which is approximated as $k * l$ (Barbour et al., 2017), in which l is the distance between the veins and the stomata in m, and k is a dimensionless scaling factor which corrects for the tortuous path, ρ_{lw} is the density of liquid water $\mathrm{g\,m^{-3}}$, and κ is the diffusivity of the heavy isotopologue in $\mathrm{m^2\,s{-}1}$ (Farquhar and Lloyd, 1993). Barbour and Farquhar (2004) determined that L = 8 mm is reasonable length scale, with l estimated at 0.1 mm.

Taking the Péclet effect into account allows the water isotopic compositions of entire leaves to be linked to the isotopic composition at the evaporation site as follows.

$$\delta_{leaf} = \frac{(1 - e^{\phi})(\delta_e - \delta_{xylem})}{\phi} + \delta_{xylem} \tag{10}$$

In reality, a series of Péclet effects, with multiple unique Péclet numbers takes place in the apoplastic cell tissue, minor veins, and major veins (Cernusak et al., 2016; Farquhar and Gan, 2003). Given that more complete formulations lack validation on key coefficients, Eq. 10 is generally used (Barbour et al., 2017).

2.2 The CO_2 isotopic state

In this work, we focus on the δ^{18}O isotopic state or *isotopic cascade* of CO_2 in the relevant reservoirs of the ecosystem, and on the isotopic link between CO_2 and H_2O. Our measurements also include $\delta^{13}C$ and we show the time series of $\delta^{13}C$ fluxes in Sec. 4.2, but do not investigate $\delta^{13}C$ in the individual reservoirs. The reason for this is that $\delta^{13}C$ has been thoroughly investigated to constrain the exchange of CO_2 on various scales (van der Velde et al., 2014; Wehr and Saleska, 2015; Oikawa et al., 2017). On global scales it has proven to be a highly valuable tracer for separating oceanic, fossil, and biospheric sources and sinks (Graven et al., 2020). At ecosystem scales however, the small isotopic disequilibrium between photosynthesis (P) and respiration (R) has been limiting for acquiring reliable partitioning results (Bowling et al., 2001; Griffis, 2013). The combined water and CO_2 isotope flux measurements performed during CloudRoots-Amazon22 provide a unique opportunity to explore the ecosystem flux partitioning using the δ^{18}O- CO_2 cycle instead.

The $\delta^{18}O$-CO_2 isotopic composition associated with assimilation

The $\delta^{18}O$ signature of CO_2 is largely determined by the isotopic composition of H_2O_l in the biosphere. Generally, the isotopic exchange between H_2O_l and $CO_{2,aq}$ is relatively inefficient, as it is dependent on the slow hydration of CO_2 ($CO_2 + H_2O \rightleftarrows$

https://doi.org/10.5194/egusphere-2025-5969
Preprint. Discussion started: 18 December 2025

$HCO_3^- + H^+$). However, the enzyme Carbonic Anhydrase (CA), readily present in plants, accelerates this exchange by 6 orders of magnitude, which allows for sub-second isotopic equilibration (Nocentini et al., 2021). The isotope exchange between liquid H_2O and CO_2 taking place as a result of hydration, is associated with a fractionation effect. Brenninkmeijer et al. (1983) determined the magnitude of this temperature dependent effect to be

$$\alpha^{18}_{H2O\rightarrow CO2} = 1 + \frac{17.604}{T} - 17.93 \times 10^{-3} \tag{11}$$

where T is the temperature in K. In vegetation, CO_2 interacts with liquid water at the liquid-gas interface in the mesophyll, where evaporation takes place. The H_2O_l isotopic composition at the exchange site (δ_e) is determined using Eq 7. The isotopic signature of CO_2 at these exchange sites (δ^{18}_c) can then be calculated by using Eq. 6, and applying $\alpha^{18}_{H2O\rightarrow CO2}$. Note that the abundance of water molecules is much larger than the abundance of CO_2 molecules which causes δ_e to be seemingly unaffected by the isotopic equilibration between H_2O_l and $CO_{2,aq}$.

To calculate the isotopic composition associated with assimilation in the canopy (δ_P), the bidirectional diffusion of CO_2 must be taken into account, in addition to the combined kinetic fractionation effects associated with transport across the stomata, the leaf boundary layer, and the atmospheric surface layer (Farquhar et al., 1993). We follow Lee et al. (2009) to solve for δ_P.

$$\delta_P = \frac{\delta^{18}_c c_i}{ci - ca} + \frac{\delta^{18}_{atm} c_a}{c_a - c_i} - \epsilon_k \tag{12}$$

Here, c_i and c_a are the CO_2 mole fraction in the intercellular air space and the atmosphere respectively $\mu\mathrm{mol\,mol^{-1}}$. During day time, photosynthetic assimilation reduces c_i compared to c_a (Farquhar et al., 1989a; González-Armas et al., 2025). Even though the net transport of CO_2 is from the atmosphere to the leaf, back diffusion through the stomata brings equilibrated CO_2 into the atmosphere. This results in an apparent fractionation that appears to take place during $\delta^{18}O$-CO_2 uptake. However, the root cause of this signal is not fractionation during uptake, but isotopic equilibration between CO_2 and H_2O followed by back-diffusion of the equilibrated CO_2 to the atmosphere.

Gillon and Yakir (2001) found that not all CO_2 molecules that undergo back-diffusion had equilibrated with the leaf water, and estimated that the extent of CO_2 hydration in leaves (θ_{eq}) of forest ecosystems was 0.96. Incorporating this effect convolutes Eq. 12 to the following (Lee et al., 2009).

$$\delta_P = \theta_{eq}(\delta^{18}_c - \delta^{18}_{atm})\frac{C_i}{Ci - Ca} - (1 - \theta_{eq})\epsilon_k \frac{C_i}{C_a} + \delta^{18}_{atm} - \epsilon_k \tag{13}$$

The $\delta^{18}O$-CO_2 isotopic composition associated with soil respiration

In the soil, the hydration of CO_2 is also the main driver affecting $\delta^{18}O$-CO_2. The availability of carbonic anhydrase (CA) in soil water is generally lower compared to the availability in mesophyll water, and related to the number and types of soil microbes (Jones et al., 2021). Wingate et al. (2009) find that complete equilibration is generally achieved in the top 5 cm. The isotopic composition of soil water samples at 5 cm depth is thus used to calculate $\delta^{18}O$-$CO_{2\,soil}$ according to Eq. 11.

https://doi.org/10.5194/egusphere-2025-5969
Preprint. Discussion started: 18 December 2025

To derive the isotopic composition of soil respiration (δ_R), the bidirectional diffusion and fractionation associated with diffusion should be taken into account, as is done for the canopy in Eq.13. Given the high concentrations of CO_2 in the soil, the effect of diffusion from the soil to the atmosphere is the dominant factor (Hashimoto et al., 2004). The formulation below takes into account the back-diffusion of air from the atmosphere into the soil (known as soil invasion; Tans, 1998).

$$\delta_R = \frac{\delta^{18}_{soil} C_s}{Cs - Ca} + \frac{\delta^{18}_{atm} C_a}{C_a - C_s} - \epsilon_{k,s} \tag{14}$$

Here, C_s is the CO_2 mole fraction of the air in the soil $\mu\mathrm{mol\,mol^{-1}}$.

3 Data collection and treatment

This study integrates data collected during the 2-week CloudRoots-Amazon22 campaign, which took place at the ATTO (Amazon Tall Tower Observatory) site in Brazil (González-Armas et al., 2025; Vilà-Guerau de Arellano et al., 2024; Moonen et al., 2025). The campaign took place during the dry season and it was characterized by days with clear skies in the morning, which developed into shallow cumulus cloud fields later in the day (de Feiter et al., 2025). Central to the isotopic δ flux measurements and associated ecosystem source compositions was an Eddy Covariance (EC) setup installed at 57 m (see Fig. 1). This height was $\approx$25 m above the canopy, and is representative for the ecosystem scale (10^5

Data acquisition rates were 20 Hz for the anemometer and the OPGA, 10 Hz for the CO_2 isotope analyser, and 4 Hz for the H_2O isotope analyser. The EC data were processed using EddyPro version 7.06 (Fratini and Mauder, 2014) (from LI-COR Inc, Lincoln, U.S.A.), and the raw output was used for evaluation. The corrections applied include double rotation of the wind fields and density corrections according to the WPL method (Wilczak et al., 2001; Webb et al., 1980). The interquartile range (IQR) of the 30 min data evaluation periods was used as an outlier filter. Here, the isotopic compositions were filtered to retain 2 times the IQR, while 3.5 times the IQR was used for mole fraction and wind field data (Moonen et al., 2023). Time synchronisation between the EC data and the isotope analysers was performed using time-lagged cross correlation on the CO_2 or H_2O mole fractions measured by both (Moonen et al., 2023). The calibration procedure for the isotope analysers is described in (Moonen et al., 2025).

In this manuscript, we focus on the analysis of composite diurnal cycles of isotopic δ fluxes and net ecosystem flux compositions. Here, data from 08-08-2022 up to and including 20-08-2022 were used. Periods of instrument instability after startup, during maintenance, or during calibrations were removed. δ fluxes were furthermore filtered for outliers, where 15×10^{-3}, 3.4×10^{-3}, and 2.2×10^{-3} $‰\,\mathrm{m\,s^{-1}}$ were the bounds for δD, δ^{18}O-H_2O, and δ^{18}O-CO_2 fluxes, respectively. The uncertainties in the δ fluxes were determined through the spectral correction method, as described in Moonen et al. (2023). The uncertainty in the δ-flux-based net ecosystem flux signature ($\delta_{...,F}$) was calculated by propagating the errors in both the net flux, and the δ fluxes. These uncertainties were limited to 30, 15, and 22 ‰ for δD, δ^{18}O-H_2O, and δ^{18}O-CO_2 respectively.

The second method we used to determine the isotopic composition of the net ecosystem flux was the Miller-Tans method. Here, the uncertainties followed from propagating the error to the slope following York (1968) (Appendix Fig. A1). The threshold was set 5$\times$ smaller for $\delta_{...,MT}$ compared to $\delta_{...,F}$, as the type of error is different.

https://doi.org/10.5194/egusphere-2025-5969
Preprint. Discussion started: 18 December 2025

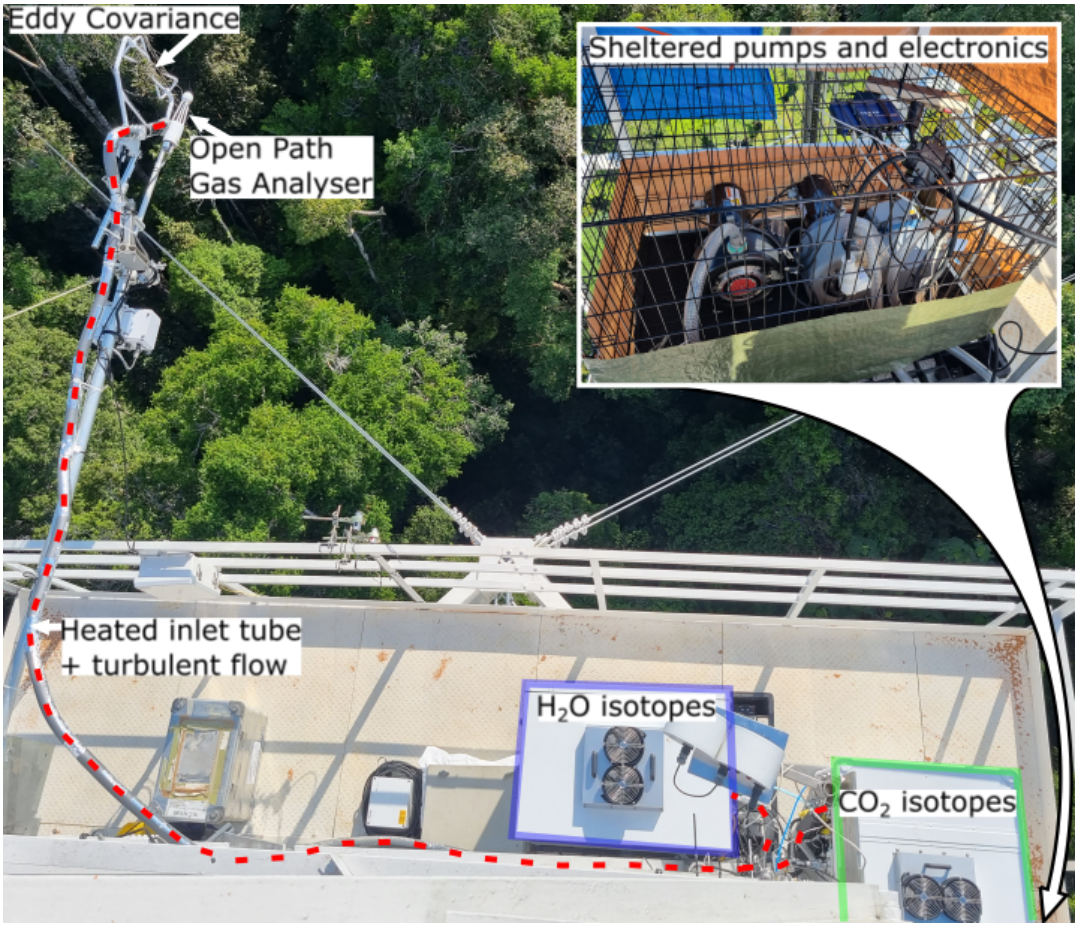

Figure 1. Picture of the isotope flux setup which was installed on the 54 m balcony of the ATTO tower in Central Amazonia, Brasil. The schematic overlay highlights the key components of the setup. The picture was taken by Oscar Hartogensis (oscar.hartogensis@wur.nl).

Finally, the difference between the ET and atmospheric isotopic compositions (δ_{ET} - δ_{atm}) was limited to the ranges -20:70, and -16:26 ‰ for δD, δ^{18}O-H_2O, respectively, and δ_{NEE} - δ_{atm} to -75:75 for δ^{18}O-CO_2, in order to exclude outliers (see Fig. 3 and 5).

3.1 Ancillary data

Besides describing a representative diurnal cycle, we describe the isotopic state of the entire ecosystem in depth at 14:00. Our reason to select this period, is that fluxes are largest, the boundary layer has fully developed and the vegetation has reached isotopic steady state (Spiridonov and Ćurić, 2021; Farquhar and Cernusak, 2005). Here we use additional isotopic information from leaf and soil samples collected from 12-08-2022 to 15-08-2022, which are described in Moonen et al. (2025). For the leaves, samples taken from the canopy top (30 m) or the middle of the canopy between 12:00 and 16:00, were averaged to

https://doi.org/10.5194/egusphere-2025-5969
Preprint. Discussion started: 18 December 2025

represent the 14:00 isotopic state. Soil samples were assumed not to vary in isotopic composition during the day. Here, the topsoil represents depths between 0-10 cm, and the deep soil depths between 40 - 100 cm.

Averaged afternoon profile data of wind speed, relative humidity, CO_2 mole fractions, and temperature were used to accurately describe the environmental conditions near the leaves and the soil (González-Armas et al., 2025). Soil temperatures were measured at three locations, and the averaged 14:00 temperature was used for our analysis.

Finally, measurements of atmospheric $\delta^{18}O$-CO_2 compositions from flask samples were incorporated. In total, the data from 22 flasks were used to determine a representative 14:00 value. These were collected from air sampling inlets on the ATTO tower ranging from 50 to 312 m and collected during the early afternoon (12:00 and 16:00) on 14-08-2022 and 15-08-2022. The data from the CO_2 isotope analyser could not be used to determine the background isotopic composition as it was unstable.

For the atmospheric compositions, δ fluxes, and ecosystem source compositions, the uncertainty associated with the 14:00 values represent the variability over the 13 composite days, expressed as the standard deviation (std). In the case of leaf and soil samples, the uncertainty is the standard error of the mean (sem) of the samples. The uncertainty in δ_R is determined by propagating the sem in the topsoil water samples. For δ_P, we instead based its error on its sensitivity to c_i/c_a, where we assume that the ecosystem wide c_i/c_a was determined with a 0.01 error (see Fig.8).

4 Results

4.1 H_2O δ fluxes and source compositions

Fig. 2 shows the composite diurnal cycle of the 57 m H_2O flux. We find a strong evapotranspiration flux during daytime, matching the period of solar irradiation (sunrise: 06:04, sunset: 18:04). Nighttime fluxes were close to zero, reflecting the reduction in turbulent transport and lack of available energy for evapotranspiration. The magnitude of the uncorrected moisture flux derived using the water isotope analyser was 9.9% smaller compared to the one derived with the conventional Open Path Gas Analyser (OPGA). Previously, water isotope flux studies have reported differences of tens of percent, indicating that we captured the high frequency contributions to the turbulent exchange flux reasonably well (Wahl et al., 2021; Moonen et al., 2023).

The diurnal cycles of the δ fluxes have a very similar shape compared to the evapotranspiration flux. The variability over the days was somewhat larger however for the δ fluxes, as shown by the 25 $\%$ and 75 $\%$ quantiles (shaded). We applied the spectral correction method described in Moonen et al. (2023) to compensate for possible high frequency signal loss. Here, the cospectral power of frequencies lower than 8×10^{-2} Hz were used to estimate the cospectral power of the highest frequencies contributing to the flux. The black dotted line in the bottom two panels indicates the impact of this correction.

For δD, the magnitudes of the fluxes with and without spectral correction are effectively equal, indicating small high frequency signal attenuation. This finding was confirmed by the $w' - H_2O'$ cospectra related to the moisture flux. For δ^{18}O, the spectral correction added 15.5 $\%$ to the flux, suggesting that there was a loss of high frequency signal for H_2^{18}O. As attenuation is generally comparable for the various H_2O isotopologues, this was unexpected. Investigating the cospectra revealed that for

https://doi.org/10.5194/egusphere-2025-5969
Preprint. Discussion started: 18 December 2025

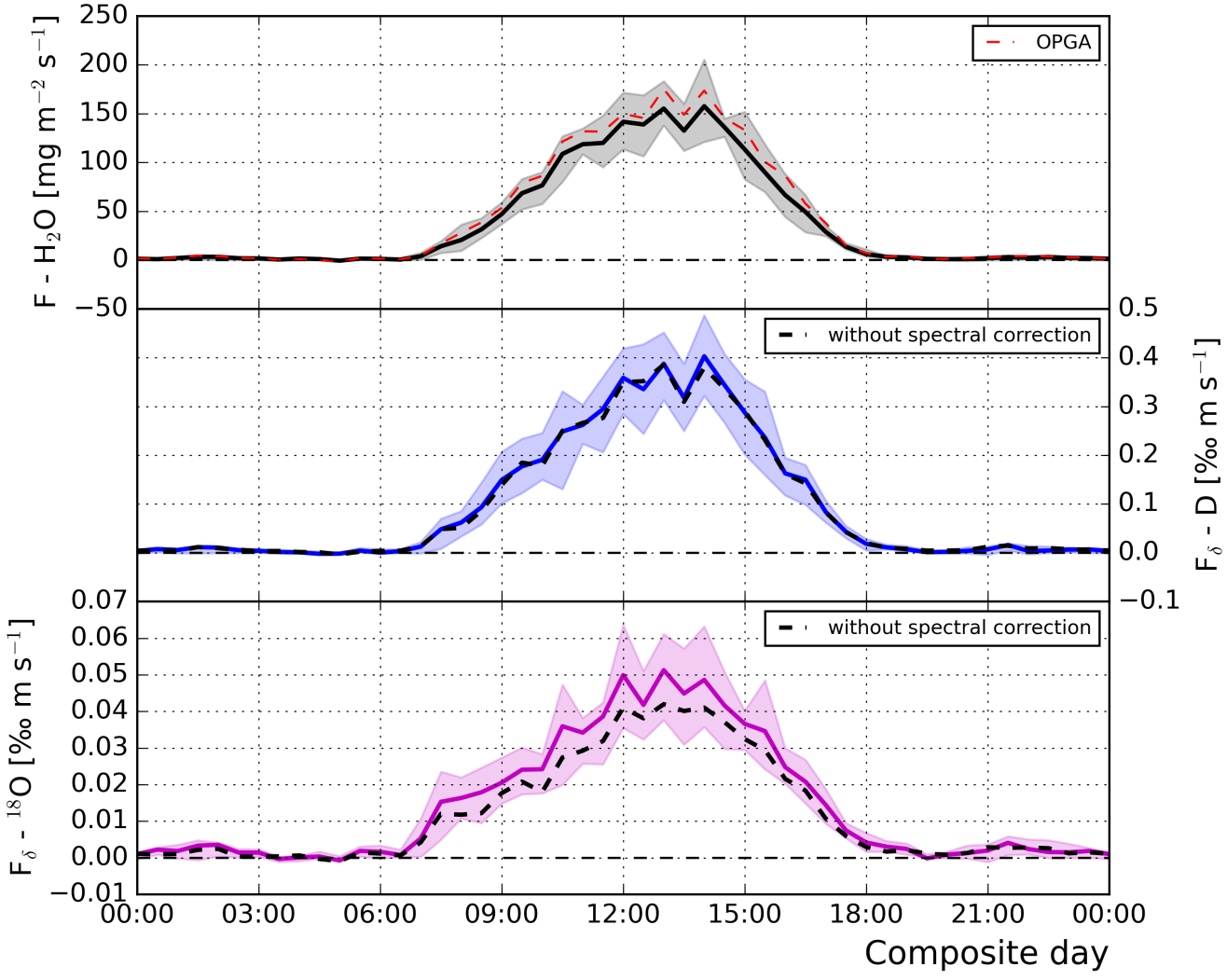

Figure 2. a) Composite day water flux derived using the closed path isotope analyser and an Open Path Gas Analyser (OPGA, shown in red). b) and c) Composite day 30 min D and ^{18}O isotope fluxes derived using the water isotope analyser combined with the EC method. The dashed black lines show the data before correction of signal loss at high frequencies. The shaded areas indicate the 25 to 75 % quantiles of the 13 days contributing to the composite day.

δ^{18}O, most frequencies contributed to the positive isotope flux as expected, but the highest frequency eddies had negative contributions. The reason for this phenomenon could not be identified.

Fig. 3 shows the composite day overview of the isotopic composition of the net ET flux (δ_{ET}) derived using the Miller-Tans ($\delta_{ET,MT}$) and Flux ($\delta_{ET,F}$) methods. For δ^{18}O as well as for δD, we find that δ_{ET} is always enriched compared to δ_{atm}. During nighttime, the isotopic composition of the net flux is highly variable over time for both species. For the flux method, this

https://doi.org/10.5194/egusphere-2025-5969
Preprint. Discussion started: 18 December 2025

is directly related to the very small (near-zero) water vapour and δ fluxes shown in Fig. 2. Eq 4 clarifies that a large uncertainty for the fluxes leads to poor estimates for $\delta_{ET,F}$. For the Miller-Tans method, the small perturbations in isotopic compositions and mole fractions associated with stable nighttime conditions also lead to large uncertain $\delta_{ET,MT}$ estimates. Moreover, these stable conditions lead to horizontally heterogeneous conditions in the forest, which results in variability between the different nights (Botía et al., 2020). During daytime, the isotopic compositions of the net exchange are instead well defined, with little variability between the contributing days.

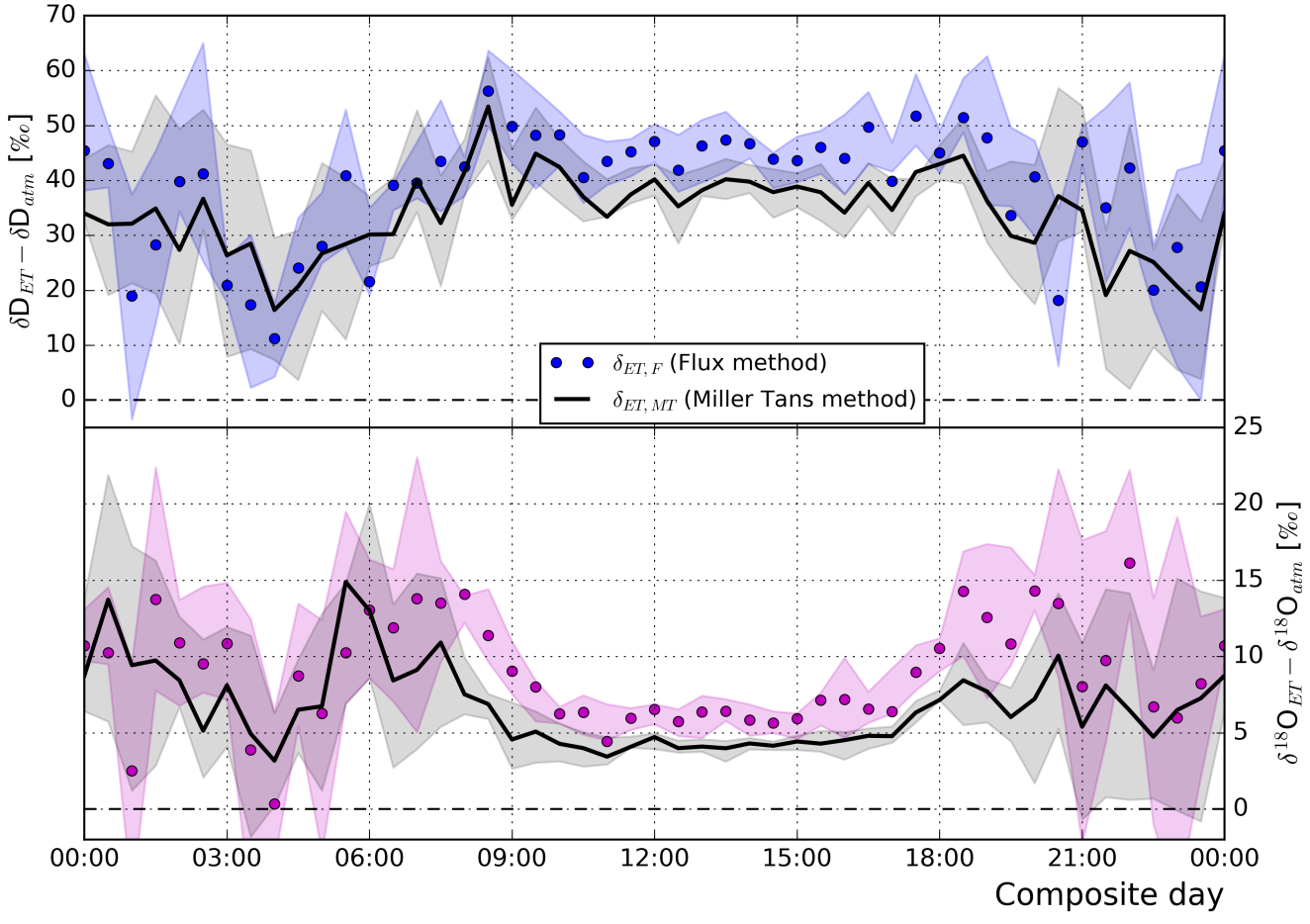

Figure 3. Composite day representation of 30 min isotopic compositions of the net flux (δ_{ET}) derived using measurements performed with the water isotope analyser. The flux method composition ($\delta_{ET,F}$) was derived using Eq. 4. Both the Miller-Tans and flux methods are described in Sec. 2. The shaded areas indicate the 25 to 75 % quantiles of the 13 days contributing to the composite day.

From 10:00 to 17:00 we find that δ_{ET} is quite constant, with a 40 ‰ enrichment for δD, and a 5 ‰ enrichment in δ^{18}O compared to the ambient atmospheric water vapour. This is consistent with the evapotranspiration of comparatively enriched water from the ecosystem to the atmosphere. For both δ^{18}O and δD we observe that net flux compositions obtained with the

https://doi.org/10.5194/egusphere-2025-5969
Preprint. Discussion started: 18 December 2025

flux method ($\delta_{ET,F}$) are more enriched than those derived from the Miller-Tans method ($\delta_{ET,MT}$) during the same period. On average, the difference is 6.4 ‰ for δD and 1.9 ‰ for δ^{18}O. The causes of this difference and the implications for the partitioning of ET are discussed in Sec. 5.1.

4.2 CO_2 δ fluxes and net flux compositions

In Fig 4, the CO_2 flux and corresponding isotope flux measurements are summarised. The NEE flux in the top panel indicates strong negative CO_2 flux during daytime, indicating photosynthetic uptake. Immediately after sunrise, however, a small positive CO_2 was observed. We interpret this positive flux to be related to the nighttime respiratory flux, which feeds CO_2 into the nocturnal boundary layer (Dupont et al., 2024). As this layer is stably stratified due to the radiative cooling of the surface, the CO_2 is trapped in the atmospheric layer below the 57 m measurement height, which includes the entire canopy. When the stability is broken after sunrise, this accumulated respiratory CO_2 is transported upward to the boundary layer and across the measurement location.

The fluxes derived with the closed path CO_2 isotope analyser compare very well to the OPGA, without any notable signal loss. The δ fluxes can thus also be expected to be resolved well. In terms of diurnal pattern, the δ flux of δ^{13}C is a mirror image of the NEE flux, including the release of trapped nocturnal respiration after sunrise. During nighttime, both the ^{13}C δ flux and NEE show a near continuous respiration flux, which is unlike the near zero fluxes for ET and δ^{18}O-CO_2.

The ^{18}O-CO_2 δ flux has a diurnal pattern which is more similar to the ET and water isotope δ fluxes. The main difference is the time from which the flux becomes positive, which is delayed by 1.5 h for ^{18}O-CO_2. The effect of the spectral corrections is similar for both δ^{13}C and δ^{18}O, although somewhat stronger for δ^{18}O. Here, the method described in Moonen et al. (2023) was primarily used to correct for instrument instabilities at frequencies lower than 9×10^{-4} Hz. Since the instrument instability increased the variability of the isotopic signals, and thus increased the magnitude of the flux, the spectral correction method leads to smaller δ fluxes for CO_2.

Fig. 5 shows the composite day overview of the isotopic composition of the NEE flux (δ_{NEE}) derived using the flux ($\delta_{NEE,F}$) method. While for H_2O the source composition can be interpreted as the composition being mixed into the atmosphere, this is not as self evident for CO_2. This is because the net exchange of CO_2 transitions from positive values during nighttime (R) to negative values during daytime (P and R). Following Eq 4, the net ecosystem flux composition must be interpreted in line with the flux direction. Thus during daytime it represents the isotopic composition of the uptake flux. For δ^{13}C, this means that we find source compositions which are depleted by 20‰ compared to the atmosphere during both day and nighttime (see Fig. 5). At nighttime, this represents the signature of respiration from decomposing organic matter. During daytime, the isotopic signature of the assimilated CO_2 is measured, which reflects the preferential uptake of depleted carbon by C3 vegetation (trees). Note that during daytime, contributions from the depleted respiration flux are also present.

The ^{18}O isotopic composition of the NEE is approximately -15‰ lower than the one of ambient atmospheric CO_2 during the night, and this difference steadily increases to -50‰ in the late afternoon. As explained above, this is an *apparent* fractionation that does not represent the fractionation associated with physical CO_2 uptake, but it is due to back diffusion of CO_2 after isotopic exchange with water. Thus, it is necessary to consider the δ^{18}O of the water with which CO_2 equilibrates in the leaves.

https://doi.org/10.5194/egusphere-2025-5969
Preprint. Discussion started: 18 December 2025

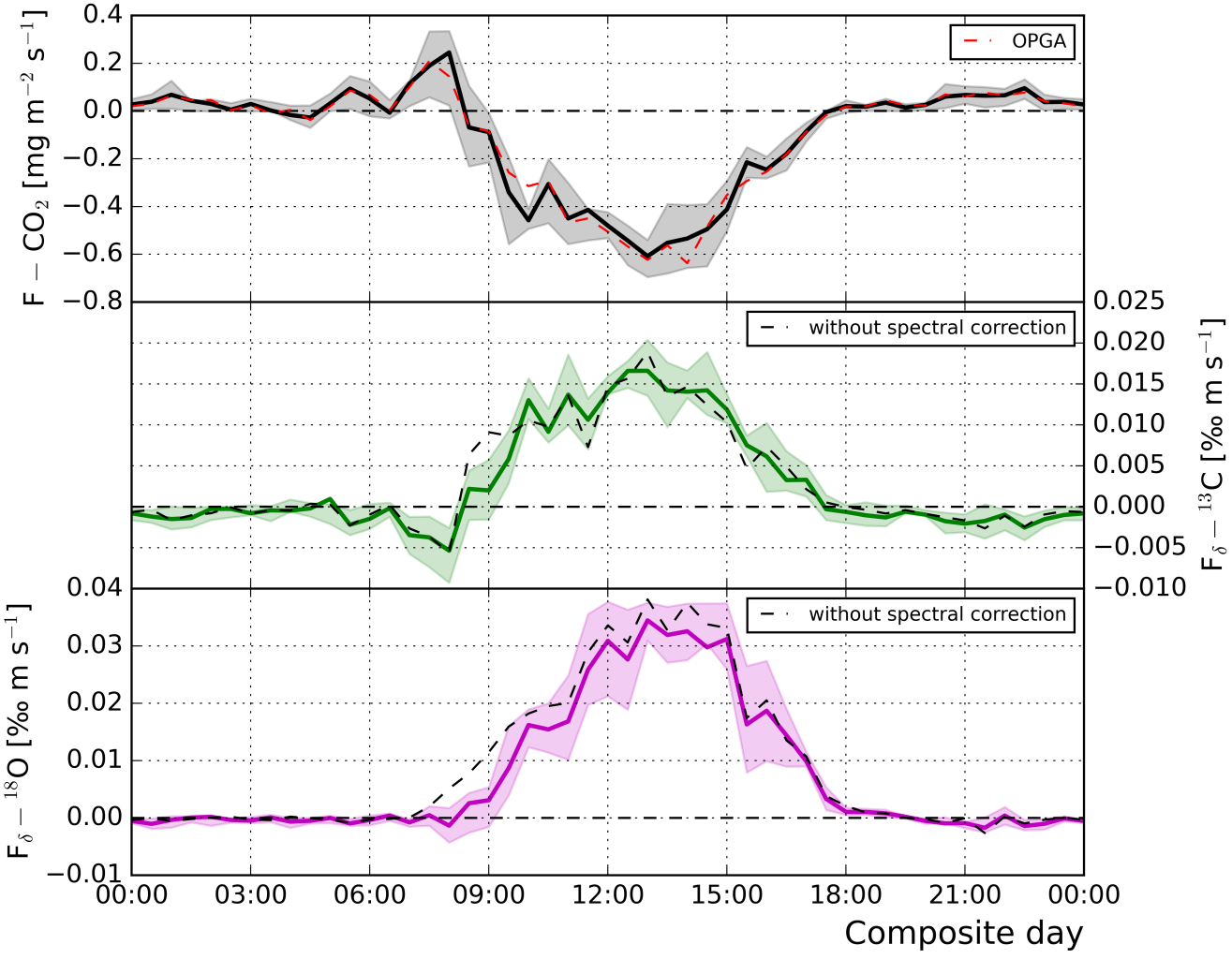

Figure 4. a) Composite day CO_2 flux derived using the closed path isotope analyser and an Open Path Gas Analyser (OPGA, shown in red). b) and c) Composite day 30 min ^{13}C and ^{18}O isotope fluxes derived using the CO_2 isotope analyser combined with the EC method. The dashed black lines show the data before correction of signal loss at high frequencies. The shaded areas indicate the 25 to 75 % quantiles of the 13 days contributing to the composite day.

During nighttime, leaf water is strongly depleted in $\delta^{18}O$ compared to daytime, which leads to respired CO_2 being depleted in $\delta^{18}O$ compared to atmospheric CO_2 (see Tab A2). This $\delta^{18}O$ depletion is indeed observed at night. During daytime, $\delta^{18}O$ in leaves gradually increases due to evaporative enrichment. As a consequence, the CO_2 molecules that exchange isotopes with water and are partially assimilated must also be comparatively enriched in ^{18}O.

So, why do we then observe a continuous depletion in $\delta^{18}O_{NEE}$ compared to the atmospheric $\delta^{18}O$ value? This is due to the net uptake of CO_2 during daytime (negative CO_2 flux), combined with the substantial diffusion of equilibrated and

https://doi.org/10.5194/egusphere-2025-5969
Preprint. Discussion started: 18 December 2025

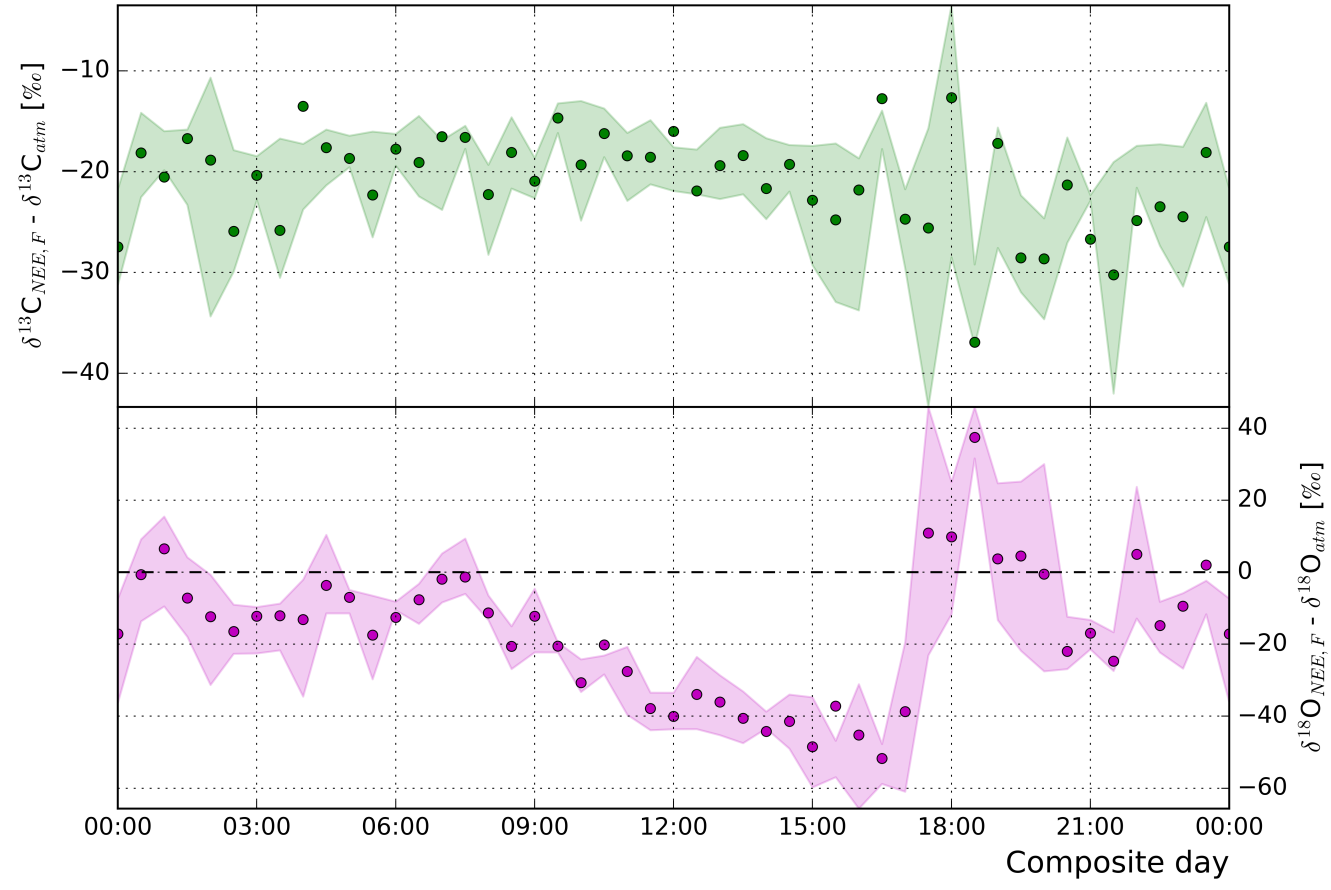

Figure 5. Composite day representation of 30 min isotopic compositions of the net CO_2 flux (δ_{NEE}) derived using the CO_2 isotope analyser. δ_{NEE} was derived using the flux method ($\delta_{...,F}$), following Eq 4. The shaded areas indicate the 25 to 75 % quantiles of the 13 days contributing to the composite day.

thus isotopically enriched CO_2 back into the atmosphere (Adnew et al., 2020). The latter effect is dominantly responsible for affecting the atmospheric isotopic composition of CO_2. However the (apparent) composition of the net uptake flux is what is determined. In our case, this net uptake flux seemingly strongly favours ^{16}O, as it enriches the atmosphere in ^{18}O, which results in a negative $\delta^{18}_F O$ (Farquhar and Lloyd, 1993; Adnew et al., 2021). The strongly depleted $\delta^{18}O$ composition of the daytime carbon flux is thus a consequence of the enrichment of the atmosphere due to back-diffusion. This apparent fractionation effect during photosynthetic uptake is further explored in Sec. 4.4.

During the transition to nighttime respiration, leaf water remains temporarily enriched in ^{18}O, which leads to the enriched source signature visible between 17:30 and 20:00. Here, the NEE and δ flux are near zero, leading to more variability between the days, as indicated by the shaded area. Compared to the highly variable nighttime source compositions for H_2O, the source compositions for the CO_2 isotopes are better defined during the night. This is because there are still significant net exchange

https://doi.org/10.5194/egusphere-2025-5969
Preprint. Discussion started: 18 December 2025

fluxes and isotope fluxes during nighttime. During the morning, the transition between the respiration peak and the onset of photosynthesis is more abrupt than during the evening transition, which allows for the source compositions to be well estimated comparatively during that time. During the evening transition around 18:00, when the sign of the net exchange flux changes to the respiration dominant nighttime, some erratic NEE isotopic signatures are also found in ^{13}C.

4.3 The H_2O isotopic state

We investigated the isotopic signatures of H_2O in water reservoirs that are relevant for the exchange of water (and CO_2) around the ATTO tower. Here, we describe the isotopic compositions within the soil, canopy, and atmospheric reservoirs, as well as the isotopic composition of the associated vertical water vapour flux as measured above the canopy. The isotopic compositions of reservoirs which were not measured directly and of individual gross fluxes were then derived following Sec. 2. The result is a coherent and connected *isotopic cascade* throughout the Amazonian ecosystem. We describe the 14:00 (LT) case which ensures that the ABL is fully developed and that isotopic steady-state has set in. To limit the effect of the sub-diurnal and inter-diurnal variability, the 14:00 case was derived from a 13-day composite diurnal cycle.

Table 1 specifies the typical environmental conditions at 14:00 at the ATTO site. These variables are key inputs for describing the isotopic H_2O and CO_2 balances. For a rainforest, the RH of 58 % within the canopy is relatively low. Note that the campaign took place during the dry season, and that only two significant rain events took place during the 13-day campaign. In addition, temperatures are highest around 14:00, contributing to a reduced RH. As a consequence, the vegetation limits evaporation by reducing its stomatal apertures, resulting in a comparatively high stomatal resistance R_s during this time. In line with this, the c_i/c_a is at a daily low at 14:00.

Table 1. Multi-day averaged 14:00 environmental and biospheric conditions during the CloudRoots-Amazon22 campaign at the ATTO site. The in-canopy scalar data and leaf gas exchange measurements were presented and interpreted in González-Armas et al. (2025).

Environmental variables	Bulk canopy (≈25 m)
RH (relative humidity from in-canopy profiles)	0.58
c_i/c_a (CO_2 concentration ratio from leaf gas exchange measurements)	0.79
c_s/c_a (CO_2 soil concentration ratio, c_s at -5 cm, following Hashimoto et al., 2004)	10
T_{leaf} (air temperature from in canopy profiles)	33 °C
T_s (soil temperature averaged from soil chambers)	26.5 °C
R_s (stomatal resistance from leaf gas exchange measurements)	136 s m^{-1}
R_b (boundary layer resistance, dependent on U, following Bonan, 2002)	77 s m^{-1}

The right hand side of Fig. 6 specifies the isotopic state of water in all the relevant reservoirs for both δD and $\delta^{18}O$. Here, we combined atmospheric observations, flux measurements, and leaf and soil level measurements (also see Table A1). Two flux pathways are highlighted by which water vapour is fed to the atmosphere: (soil) evaporation and transpiration, respectively. Here, the transpired water (δ_T) is enriched compared to the atmospheric reservoir (δ_{atm}), whereas the evaporated water δ_E is

https://doi.org/10.5194/egusphere-2025-5969
Preprint. Discussion started: 18 December 2025

depleted compared to δ_{atm}. This difference is key to resolve, as it allows us to partition the net ET flux into the components E and T in Sec. 4.5.

Ultimately, the source water of both evaporation and transpiration is the same, namely precipitation. While there is some seasonal variability in the isotopic composition of precipitation, with the wet season feeding more depleted water to the ecosystem, this will not impact our 13 d measurement campaign (Zhiña et al., 2022). The isotopic composition of topsoil water (δ_{soil}) is determined by the composition of recent precipitation and the accumulated effect of the evaporative enrichment of the near-surface water reservoir due to Rayleigh fractionation. The latter effect results in the topsoil water to be more enriched compared to the water below (see Fig. 6). Compared to δ_{soil}, the evaporated water δ_E is strongly depleted due to the preferential evaporation of HHO compared to HDO (Horita and Wesolowski, 1994).

As explained above, the isotopic composition of transpiration (δ_T) is assumed to be identical to δ_{xylem} because of mass conservation (Dongmann et al., 1974). As a result, the isotopic composition of transpired water vapour (δ_T) is much more enriched than δ_E. The Craig-Gordon model (Eq. 7) allows to determine the isotopic composition of liquid water at the exchange site (δ_e) that is required to supply these high values of δ_T. The results representing our study case are shown in Fig. 6: $\delta^{18}O_e$ is 15‰ higher than $\delta^{18}O_{xylem}$, while δD_e is more than 50‰ more enriched than δD_{xylem}. δ_{lam}, the isotopic composition of water in the leaf lamina, illustrates that this enrichment occurs only locally within the leaf as a consequence of the Péclet effect (see Eq. 9). Liquid water samples of entire leaves (δ_L), which comprise both the leaf veins and the leaf lamina, bridge the composition of the enriched evaporation sites, and the comparatively depleted δ_{xylem} source water (Cernusak et al., 2016). Table A1 specifies the important intermediate steps in the isotopic cascade, and also provides the uncertainties for some of the variables.

4.4 The CO_2 isotopic state

The left hand side of Fig. 6 specifies the 13 day averaged 14:00 isotopic state for δ^{18}O-CO_2. Similar to H_2O, two flux pathways are highlighted which together determine NEE, namely the (soil) respiration flux (R) and the photosynthetic assimilation flux (P). Importantly, the isotopic exchange of ^{18}O-CO_2 is controlled by the isotopic composition of H_2O throughout the ecosystem, which means that tight links between the left and right hand sides of Fig. 6 exist.

The isotopic composition of assimilated CO_2 (δ_P) is apparently strongly depleted in ^{18}O compared to δ_{atm}. This is a particularly important and counter-intuitive effect in the δ^{18}O-CO_2 cascade, and it results from the isotopic exchange between CO_2 and H_2O in the mesophyll of leaves. Oxygen isotopes are exchanged so quickly between CO_2 and H_2O that the isotopic composition of CO_2 in the stomata is generally believed to be in isotopic equilibrium with the H_2O at the site of exchange (Farquhar and Lloyd, 1993). This means that the δ^{18}O-CO_2 in the stomata is decoupled from the isotopic composition of ambient CO_2, and in our case enriched (see δ_c). As mentioned above, part of this isotopically enriched CO_2 diffuses back through the stomata into the atmosphere, and isotopically enriches that reservoir. The net effect of the CO_2 exchange through the stomata is (photosynthetic) uptake however, so the atmosphere close to the leaf does have lowered CO_2 mole fractions. The combination of the net uptake and the back-diffusion of ^{18}O- enriched CO_2 makes it seem as though ^{16}O-CO_2 is apparently

https://doi.org/10.5194/egusphere-2025-5969
Preprint. Discussion started: 18 December 2025

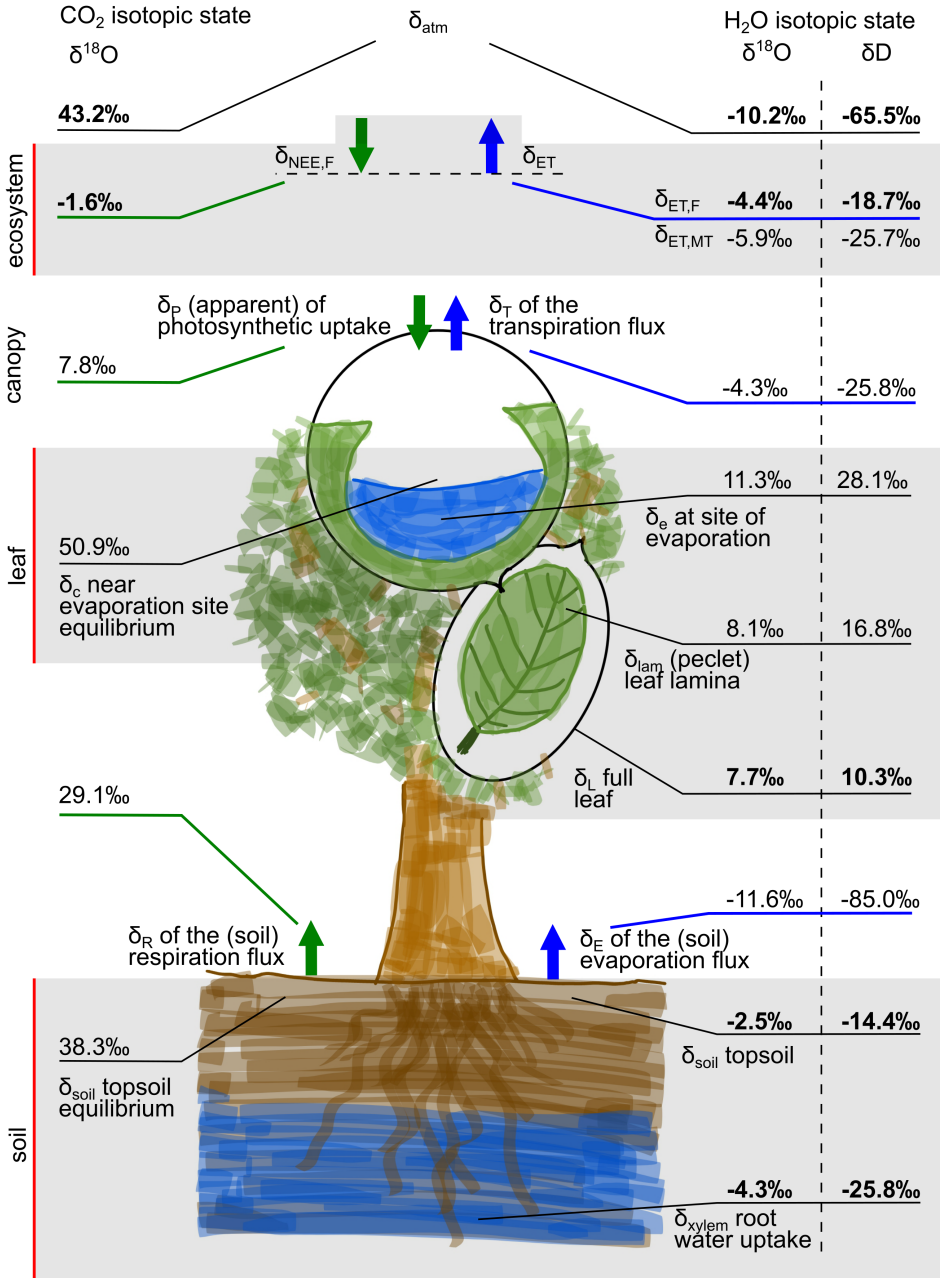

Figure 6. Overview of the CO_2 and H_2O isotopic state of the Amazon rainforest ecosystem, representative for the average 14:00 conditions at the ATTO site during the CloudRoots-Amazon22 field campaign. Bold font indicates that the variables were derived from measurements. The vertical text highlights the scale which a certain set of variables grouped by shade/no-shade represents. The uncertainties associated with the values are provided in Tab. A2 and A1 of the appendix, if available.

https://doi.org/10.5194/egusphere-2025-5969
Preprint. Discussion started: 18 December 2025

assimilated faster than ^{18}O-CO_2. It is important to realize that this is not a physical fractionation effect, but an apparent fractionation effect (Adnew et al., 2020).

δ_P-δ_{atm} indicates the strength of the *apparent* fractionation effect, which is -35 ‰. This difference is larger than what might be expected given the isotopic composition near the exchange sites (δ_e) in the mesophyll (δ_c-δ_{atm}) of about 8 ‰. In Sec. 4.5 we detail how this amplification emerges in relation to the c_i/c_a ratio, which determines the relative strength of the back-diffusion. This effect turns out to be key for partitioning NEE. In contrast to δ_P, the isotopic composition of respired CO_2 (δ_R) is only weakly depleted relative to δ_{atm} (-14.1 ‰).

The source signature of the soil respiration flux (δ_R) is primarily affected by equilibration with the soil water isotopic composition. Any CO_2 in the soil, whether it has been locally respired or invaded from the atmosphere, equilibrates with topsoil H_2O_l (δ_{soil}^{liq}, Wingate et al., 2009). During the subsequent diffusion from the soil into the atmosphere, the CO_2 from the soil ($\delta_{soil}^{CO_2}$) undergoes kinetic fractionation (Tab. A2). This results in a depletion of the isotopic composition of the respiration flux (δ_R) compared to δ_{soil}^{CO2}. In addition, invasion of CO_2 into the soil and subsequent back diffusion into the atmosphere has a depleting effect. However, as the concentration of CO_2 in a tropical rain forest soil is much higher then in the atmosphere, this effect is comparatively small (Hashimoto et al., 2004).

In total, the enriching effect of δ_P on δ_{atm} is larger than the depleting effect of δ_R, which results in the net positive δ^{18}O-flux we observe in Fig. 4. In line with this, and given that the NEE flux is negative, the isotopic composition of this flux ($\delta_{NEE,F}$) is depleted compared to the atmospheric background. Using our measurements and Eq. 4, $\delta_{NEE,F}$ was determined as -1.6‰. This is lower than both the canopy and the soil flux end-members δ_P and δ_R, which can seem illogical. This is, however, a mathematical effect of attributing the depletion associated with both gross fluxes to one smaller net flux. In fact, we show below that the derived value of $\delta_{NEE,F}$ does allow for the flux partitioning equations to be solved (Sec. 4.5), and it is in line with previously measured values by, for example, Griffis (2013), who found a $\delta_{NEE,F}$ of -10.5 ‰ above a soybean field.

4.5 Net ecosystem flux partitioning

The values established in previous sections can be used to partition the measured net ecosystem exchange fluxes NEE for CO_2 and ET for H_2O into the individual gross flux components according to Eq 2. δ_{ET} was taken as the average of the values determined from the direct flux measurements $\delta_{ET,F}$ and the Miller-Tans mass balance approach $\delta_{ET,MT}$. δ_E was assumed to equal δ_{soil}^{vap}, and δ_T was represented by δ_{xyl} (see Sec. 2.1). Using the average of the partitioning results derived from δD and δ^{18}O, we find that the transpiration flux (T) contributes 95.5% to ET at 14:00 on average (Fig. 7). A dominant contribution of T is expected given the high uptake of radiation by the canopy crown and resulting shading in the understory (González-Armas et al., 2025). The 4.5% contribution from soil evaporation flux (E) is an important finding, as few studies have attempted to estimate the soil contributions, and it is assumed in many studies that no soil evaporation takes place at all (Belk et al., 2007; Schellekens et al., 2000; Malhi et al., 2002). Note that ET partitioning using δD only results in $E = 0$, as δD_{ET} is even more enriched than δD_T according to our measurements.

For the NEE flux, the partitioning suggests that P is 144% of NEE, which is compensated by an R of -44% of NEE (Fig. 7). We found that this result was strongly dependent on the component δ_P, which is the apparent isotopic composition of

https://doi.org/10.5194/egusphere-2025-5969
Preprint. Discussion started: 18 December 2025

P. Given its origin from CO_2 back-diffusion, the strength of δ_P depends on c_i/c_a. For the value we used (c_i/c_a = 0.79) we find δ_P = 7.8 ‰. To interpret δ_P, it helps to consider c_i/c_a as describing a balance of fluxes ($F_{out}/F_{in} = \frac{ci/ca}{1-ci/ca}$). The value of 0.79 means that for every CO_2 molecule being assimilated, roughly 4 CO_2 molecules diffuse back into the atmosphere. This illustrates that while the enriching effect on the atmosphere is not large per back-diffusing molecule (see Fig. 6), the effect is leveraged 4 fold when interpreting it as an uptake fractionation effect. In Sec. 5 and Fig. 8 we explore the sensitivity of the partitioning result to this uptake fractionation leveraged by c_i/c_a.

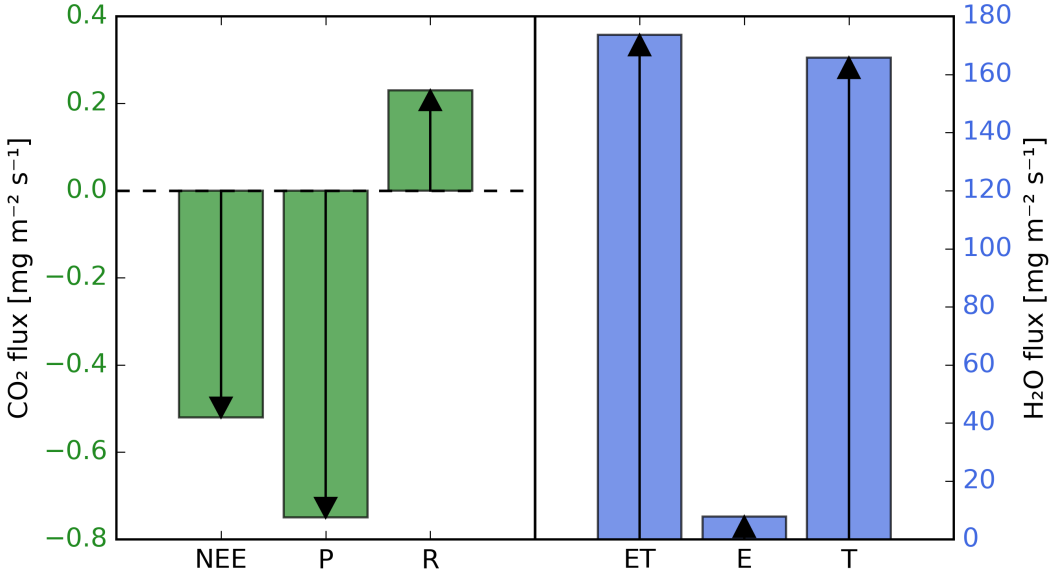

Figure 7. Results of the partitioning of the net ecosystem exchange fluxes NEE and ET using stable isotopes, following Eq 2. For NEE, the ^{18}O-CO_2 isotope was used following the approach described in Sec. 2.2. For ET, the average of the partitioning results derived from δD and δ^{18}O is shown (see Sec. 2.1).

The uncertainty in the partitioning result is determined by the uncertainties in the net ecosystem fluxes (ET and NEE), the isotopic end-members (δ_E, δ_T, δ_R, and δ_P), and the derived isotopic composition of the net ecosystem fluxes (δ_{ET} and δ_{NEE}). Here, the uncertainties in the isotopic components can be assumed to be largest. In tables A1 and A2 we provide the estimated errors in all of these isotopic components. Note however, that the various types of errors are not directly comparable. For example, the large uncertainties in δ_{ET} and δ_{NEE}, which indicate the variability (std) in these variables over the 13 composite days, are likely smaller than the end-member compositions (sem) when considering the instantaneous 14:00 afternoon case we analyse (see Sec. 3.1). As a result, we have not explicitly determined uncertainties for the partitioning results.

https://doi.org/10.5194/egusphere-2025-5969
Preprint. Discussion started: 18 December 2025

5 Discussion

We have used in-situ measurements of CO_2 and H_2O isotope fluxes far above the top of the canopy in the Amazon forest (57 m) to partition the net ecosystem fluxes of both NEE and ET into their individual components. This was possible because we could describe the complete isotopic state of $\delta^{18}O$ in both CO_2 and H_2O throughout the ecosystem by making use of additional isotopic information from leaf and soil samples. Here, we have demonstrated that the isotopic states at the evaporative sites in the leaves — where CO_2 and H_2O isotopic cascades intersect — are physically consistent between the two species. Our results give confidence that isotope flux measurements can provide reliable ecosystem scale partitioning results.

5.1 Ecosystem source compositions

As shown above, we have used high frequency isotope measurements to determine the isotopic composition of the ecosystem flux (δ_{ET} and δ_{NEE}). For δ_{ET}, two estimates were used and compared: one using the measured δ flux ($\delta_{ET,F}$) and the other one using the Miller-Tans $\delta_{ET,MT}$ method. We found that $\delta_{ET,F}$ produced systematically more enriched values, where δD was 6.4 ‰ more enriched and $\delta^{18}O$ was 1.9 ‰ more enriched compared to $\delta_{ET,MT}$. Griffis et al. (2007) also compared the $\delta_{ET,F}$ to a mixing model method, however for $\delta^{13}C$ of CO_2. They found that $\delta_{ET,F}$ was ≈ 5 ‰ more enriched, which in their case meant closer to δ_a, than $\delta_{ET,MT}$. They attributed this systematic effect to footprint differences. $\delta_{ET,F}$ indeed represents local exchange in the footprint area of the isotope and the net ecosystem flux measurements, while $\delta_{ET,MT}$ can also be influenced by other up-wind exchange processes, which affect the measured atmospheric compositions (see Fig. A1). It is not clear, however, why up-wind exchange would be much different compared to local exchange, given the homogeneity and vast scale of the Amazon rainforest ecosystem surrounding the ATTO site.

We suggest that differences between $\delta_{...,F}$ and $\delta_{...,MT}$ should be further investigated to determine which method is more appropriate for determining the isotopic composition of the ecosystem flux. For now, we speculate that the estimate from $\delta_{...,F}$ will be more reliable because (1) the footprint better matches the flux and in-ecosystem measurements we took, and (2) because the Miller-Tans method is subject to stringent assumptions which are not underlying the flux method. Here, especially the two end-member mixing assumption is likely violated, as vapour sources from an ecosystem are not isotopically uniform, but highly variable in composition (Miller and Tans, 2003; Griffis et al., 2010; Cernusak et al., 2016).

5.2 The sensitivity of ecosystem partitioning to local sampling

Determining flux partitioning at the ecosystem scale is important for linking the understanding of leaf and canopy scale processes to the scales relevant for remote sensing and modelling purposes (Gentine et al., 2019; Vilà-Guerau de Arellano et al., 2023). It is important to realize that leaf and soil water isotopic composition measurements are always necessary to determine the end members for isotopic partitioning. In addition, c_i/c_a ratios need to be known, and they are usually determined with dedicated (and labour intensive) leaf gas exchange measurements (González-Armas et al., 2025). While we attempted to capture the variation across space and species in these variables, it is challenging to obtain a subsample that is truly representative for the entire ecosystem. Moreover, such measurements are labour intensive. Once a high temporal resolution isotope flux

https://doi.org/10.5194/egusphere-2025-5969
Preprint. Discussion started: 18 December 2025

system is in place, this may be the least time consuming component of the flux partitioning system. Therefore, we consider the necessity of detailed leaf and soil scale measurements to be the major obstacle for more wide spread implementation of isotopic ecosystem scale flux partitioning.

Replacing detailed leaf and soil scale measurements with assumptions or approximations based on environmental variables is appealing for simplifying isotopic ecosystem scale flux partitioning. For example, the c_i/c_a ratio is regularly assumed to be 0.7 (Farquhar et al., 1989a). Alternatively, its value can be approximated using the stomatal conductance and the water vapour pressure deficit (Ronda et al., 2001). However, we find that the isotopic end-member δ_P is highly sensitive to the c_i/c_a ratio, which makes us believe that approximations are likely insufficient for deriving reliable partitioning values. Even with the intensive c_i/c_a monitoring during CloudRoots-Amazon22, described in González-Armas et al. (2025), we are left with some uncertainty regarding an appropriate c_i/c_a ratio. Fig. 8 indicates how this uncertainty propagates to the determination of δ_P, and what the consequences are for the NEE partitioning result.

For our observed value of c_i/c_a = 0.79, Fig. 8 indicates that an isotopic composition of the canopy uptake flux (δ_P) is found which allows for the partitioning of NEE. However, the upper bound of the possible c_i/c_a range would result in a δ_P close to the solid horizontal line, which indicates the limit of possible partitioning results, leading to a respiration flux of near zero. The lower bound of the possible c_i/c_a range, 0.77, which is only smaller by 0.05, would instead suggest a large R (-69 $\%$ of NEE), compensated by a strong P uptake flux (169 $\%$). The exact value of the ecosystem wide c_i/c_a is thus important to know. Note that the daytime averaged c_i/c_a is approximately 0.86, which does not allow for partitioning at all. To describe the ecosystem exchange, it is thus essential to resolve the diurnal cycle of variables like c_i/c_a with measurements, which allows for the diurnal dynamics to be taken into account appropriately.

5.3 Water isotopic (steady-) state

For the H_2O isotopes, the assumption of isotopic steady-state is important and much discussed (Farquhar and Cernusak, 2005; Barbour et al., 2017; Yakir and da Silveira Lobo Sternberg, 2000). This assumption implies that during continuous transpiration, a balance emerges between the isotopic composition of the water taken up by a plant, and the water vapour transpiring into the atmosphere. This results in a strong isotopic enrichment of the water at the evaporation sites in the leaves. While this assumption is adequate for longer timescale (1 mo) analysis, it has been shown to be problematic at short timescales ($<$1 d), where irregularities due to buffering and fast fluctuations in environmental conditions are observed (Cernusak et al., 2016). In our analysis we have used the steady-state Craig-Gordon model. For the 14:00 case, we do not expect the steady-state assumption to be violated, as this is the time of day where enough water has been processed through the plant, and is being transpired, for steady-state to set in (Griffis, 2013). However, if we expanded our analysis to the entire diurnal cycle - where during the night transpiration is small and the leaf evaporation sites are not enriched - the steady-state assumption would most likely not be adequate.

Non-steady-state Craig-Gordon models allow to describe diurnal dynamics better than steady state models, and would therefore be preferred for ecosystem scale flux partitioning(Craig and Gordon, 1965). However, they require independent estimation of the isotopic composition of transpired water (δ_T), without assuming that this composition is equal to the source water

https://doi.org/10.5194/egusphere-2025-5969
Preprint. Discussion started: 18 December 2025

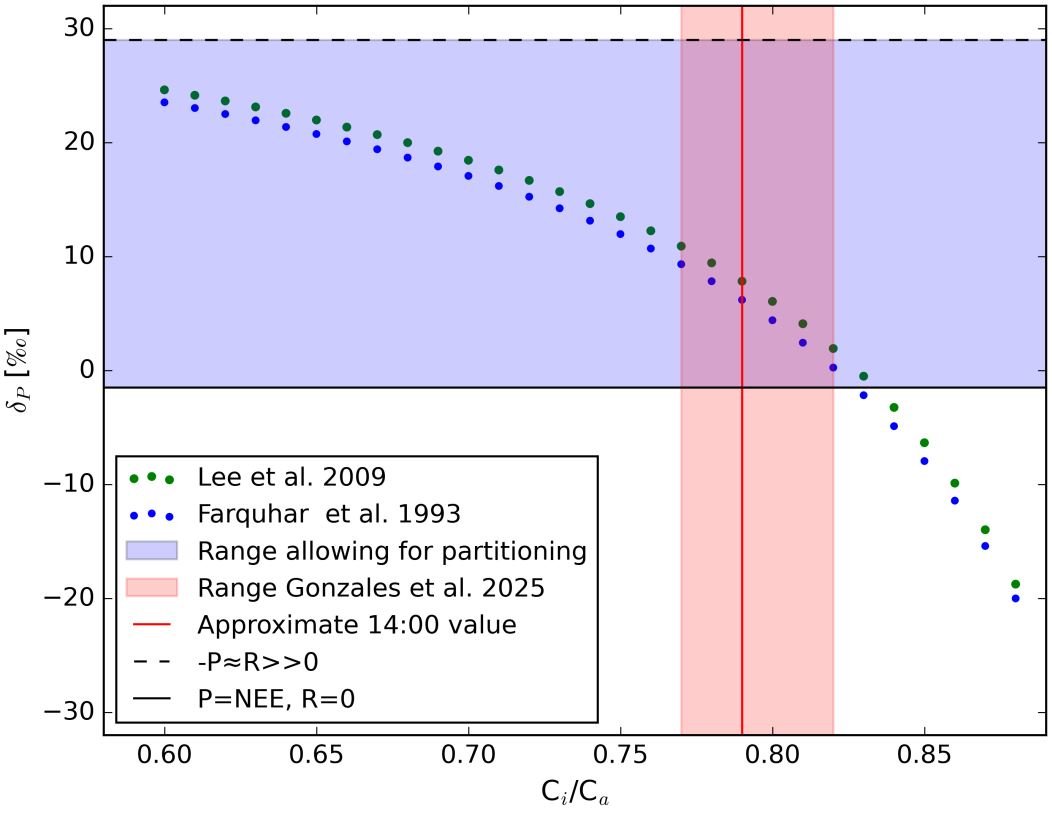

Figure 8. Simulated sensitivity of δ_P to the c_i/c_a ratio following the original mathematical formulations of Farquhar et al. (1993) and the formulation of Lee et al. (2009) in which the incomplete equilibration between H_2O and CO_2 is considered (Eq. 13. The red line and shading indicate the average value and total observed range of c_i/c_a at 14:00 (González-Armas et al., 2025). The horizontal black lines indicate the upper and lower limits of δ_P for which a partitioning result based on Eq. 2 can be found (blue range) given the isotopic composition of NEE ($\delta_{NEE,F}$ = -1.6‰) and of the soil respiration end-member (δ_{soil} = 29.1‰).

(δ_{xylem}), as we have done under the steady-state assumption. In natural ecosystems, δ_T is not only difficult to measure, it is also complex to estimate independently. Ideally, the isotopic composition of the water at the evaporation site (δ_e) would be known, so that δ_T can be solved for reliably. Direct sampling of δ_e is impossible however, as the actual sites of evaporation are microscopically small. Instead, water samples from complete leaves or leaf lamina might be used to estimate δ_e by taking into account the Péclet effect. The limit here is that the magnitude of the Péclet effect is highly dependent on the tortuosity of the water path (k, See Eq. 9). Estimates for this coefficient vary considerably between experiments and species (Barbour and Farquhar, 2004). While steady-state leaf water assumptions are thus known to be inadequate, the increased complexity of non-steady-state models is hard to take into account in natural ecosystems, posing a limit for applying the ecosystem flux partitioning technique using isotope information to the entire diurnal cycle.

https://doi.org/10.5194/egusphere-2025-5969
Preprint. Discussion started: 18 December 2025

The isotopic steady-state assumption is not applicable to soils due to the comparatively large size of the water reservoir in contact with the atmosphere (Wingate et al., 2009). This results in diffusion of enriched water from the evaporation sites back into the topsoil water pool. Over time, this results in the gradient we illustrate in Fig. 6, where the topsoil becomes enriched compared to the deep soil water. This enrichment can be expected to have a limited diurnal cycle, which allows for topsoil water samples to be used to estimate δ_E for the entire day. The topsoil water enrichment we find during CloudRoots-Amazon22 is very small, with a gradient in δD of 8.6 ‰. Canet-Martí et al. (2023) instead find gradients in δD reaching 40 ‰in agricultural fields. The resetting of the gradient by regular precipitation in the Amazon could in part explain this large difference. On top of this, the strong shading from the rainforest canopy, and leaf litter, which limit solar irradiance and thereby E, contributes to the small soil water isotopic gradients in the Amazon.

5.4 Broader perspective

The work presented in this chapter shows that isotopic flux partitioning is possible and offers insight into the individual gross fluxes. Further implementation of the method is limited by (1) the requirement for local scale sampling measurements to determine the appropriate isotopic end-members, and (2) by the methodological uncertainties and assumptions associated with the method. Still, we consider diurnally resolved individual flux estimates of the net exchange of H_2O and CO_2 to be within reach. Such insights will help to better validate and understand ecosystem behaviour (Baldocchi, 2014; Stoy et al., 2019). In addition, describing the diurnal dynamics of the isotopic reservoirs in an ecosystem would enable us to advance understanding of the isotopic budgets of H_2O and CO_2 in the atmosphere by taking into account non-linear land-atmosphere exchange effects (Farquhar and Lloyd, 1993; Gillon and Yakir, 2001; Adnew et al., 2020).

6 Conclusions

As part of the CloudRoots-Amazon22 campaign, we carried out the first simultaneous in-situ measurements of H_2O and CO_2 isotope fluxes at the ATTO site in the Central Amazon rainforest during the dry season (August 2022). In this manuscript, a 13-day composite diurnal cycle of the isotopic fluxes and the associated isotopic compositions of the net ecosystem flux was characterised. We identify pronounced diurnal dynamics which we qualitatively connect to the interacting processes governing the exchange of H_2O and CO_2. An early afternoon steady-state case (14:00 h) was compiled and combined with water isotopic composition measurements of key source reservoirs (soil, leaf), which enable the partitioning of net ecosystem fluxes into their underlying individual gross fluxes. As an intermediate step towards this goal, we have provided a complete description of the *isotopic cascades* of H_2O and CO_2 throughout the 32 m canopy, using the comprehensive soil, leaf, vertical profile, 57-m flux and ecophysiological data gathered during our campaign. Here, the δ^{18}O isotopic composition provides a key link between H_2O and CO_2, because ^{18}O is readily exchanged between both species in the biosphere according to a well established thermodynamic isotope equilibrium. The coherence between the determined isotopic states of H_2O and CO_2 at the leaf evaporative sites confirms that our isotope(-flux) measurements are physically consistent at the ecosystem scale.

https://doi.org/10.5194/egusphere-2025-5969
Preprint. Discussion started: 18 December 2025

Combined analysis of δ^{18}O and δD shows that at 14:00, transpiration dominates evapotranspiration (≈95.5 %), while soil evaporation contributes only 4.5 % to ET, consistent with the expected dominant cycling of water through plants, and the strong surface shading in tropical rainforests. Using the ^{18}O isotope of CO_2, we find that (soil) respiration accounts for -44 % of the Net Ecosystem Exchange (NEE) of CO_2, with assimilation being 44 % larger than NEE as a consequence. Here, detailed investigation of the isotope-based partitioning revealed that the apparent isotopic composition of assimilation (δ_P) is highly sensitive to the c_i/c_a ratio, highlighting the necessity for accurate leaf-level measurements to constrain canopy-scale processes.

Overall, our findings demonstrate that isotope flux measurements can bridge the gap between process-based understanding at the leaf and soil level and ecosystem-scale exchange of H_2O and CO_2. The need for independent estimates of isotopic end members of gross fluxes from the ecosystem remains a practical limitation for field applications. Yet, applying such methods across sites and seasons will help to quantify how the coupling between the carbon and water cycles responds to environmental change in the Amazon and in other ecosystems. Detailed and comprehensive observations like the ones presented here could also help to quantitatively assess the contribution of soils and plants to the diurnal variability within the context of high-resolution (100-m scale) weather and carbon cycle simulations (Pedruzo-Bagazgoitia et al., 2023).

Data availability. Data is available under open access with DOI: https://doi.org/10.6084/m9.figshare.30762821

https://doi.org/10.5194/egusphere-2025-5969
Preprint. Discussion started: 18 December 2025

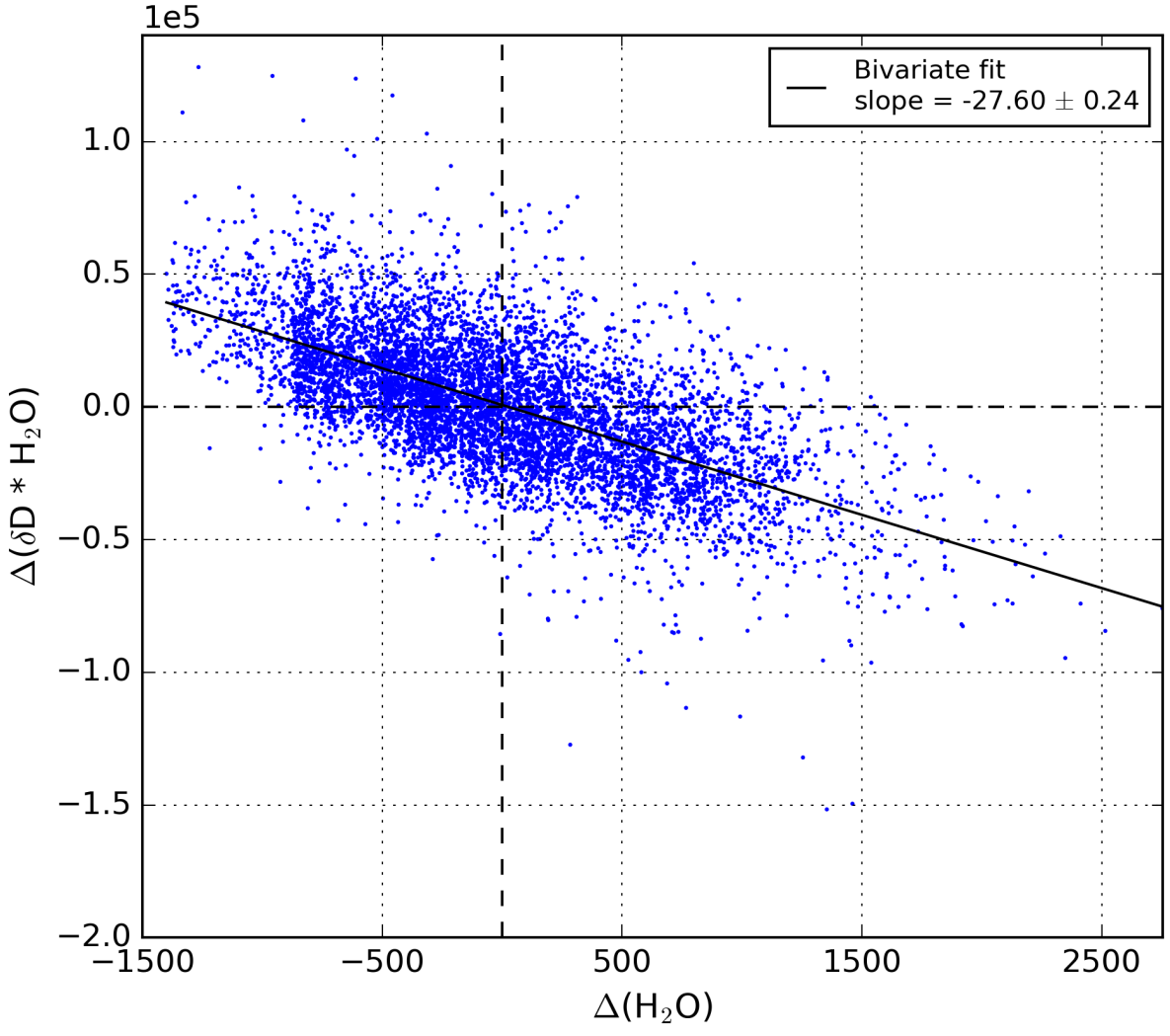

Figure A1. Example Miller-Tans analysis of the 30 min interval starting at 15:00 on 15-08-2022. The variations in δ-values and mole fractions were measured using the H_2O isotope analyser measuring from the inlet at 57 m. The Δ refers to the difference between the measured value and the atmospheric background (Miller and Tans, 2003).

https://doi.org/10.5194/egusphere-2025-5969
Preprint. Discussion started: 18 December 2025

Table A1. Overview of the H_2O isotopic state of the ecosystem, including intermediate results not shown in Fig. 6 of the main text. Related variables are grouped together. The groups follow the vertical gradient from the atmosphere to the soil water. "Type" specifies the data type, where m indicates that the variable was measured, s indicates that the variable was directly solved for, without assumptions, sa indicates that assumptions were required to solve for the variable, as described in the text.

Component of the isotopic water cycle	Type	δD	δ^{18}O
δ_{atm} (isotopic composition of atmospheric vapour)	m	-65.5 ±0.9 ‰	-10.2 ±0.12 ‰
$\delta_{ET,F}$ (isotopic composition of the ET flux from the ecosystem, following Eq. 4)	s	-18.7 ±1.4 ‰	-4.4 ±0.5 ‰
$\delta_{ET,MT}$ (isotopic composition of the ET flux from the ecosystem, following Miller and Tans, 2003)	s	-25.7 ±1.7 ‰	-5.9 ±0.18 ‰
δ_L (leaf water isotopic composition from leaf samples)	m	10.3 ±1.2 ‰	7.7 ±0.5 ‰
δ_L^{pct} (leaf water isotopic composition determined using the Péclet effect, following Eq. 10)	sa	16.8 ‰	8.1 ‰
δ_e (isotopic composition of the water exchange sites in leaves)	s	28.1 ‰	11.3 ‰
α^+ (liquid to vapour fractionation in leaves, following Horita and Wesolowski, 1994)	s	1.0706	1.0087
α_k (canopy kinetic fractionation, following Farquhar et al., 1989a)	s	1.0221	1.0247
δ_{xyl} (isotopic composition of the xylem water, derived from deep soil samples and run-off water)	m	-25.8 ±1.9 ‰	-4.3 ±0.3 ‰
δ_{soil}^{liq} (isotopic composition of liquid water in topsoil (0-10 cm) samples)	m	-14.4 ±1.8 ‰	-2.5 ±0.2 ‰
δ_E (isotopic composition of soil evaporation)	sa	-85.0 ±1.8 ‰	-11.6 ±0.2 ‰
α^+ (liquid to vapour fractionation for topsoil, following Horita and Wesolowski, 1994)	s	1.0771	1.00922

https://doi.org/10.5194/egusphere-2025-5969
Preprint. Discussion started: 18 December 2025

Table A2. Overview of the CO_2 isotopic state of the ecosystem, including intermediate results. Related variables are grouped together. The groups follow the vertical gradient from the atmosphere to the soil water. "Type" specifies the data type, where m indicates that the variable was measured, s indicates that the variable was directly solved for, without assumptions, sa indicates that assumptions were required to solve for the variable.

Component of the isotopic CO_2 cycle	Type	$\delta^{18}O$
δ_{atm} (isotopic composition of atmospheric CO_2)	m	43.2 ±0.2 ‰
$\delta_{NEE,F}$ (isotopic composition of the NEE uptake flux)	s	-1.6 ±5.4 ‰
δ_P (apparent photosynthetic uptake composition, following Lee et al., 2009)	s	7.8 ±1.7 ‰
δ_P^{Farq} (apparent canopy uptake composition, following Farquhar et al., 1993)	s	6.2 ±1.7 ‰
α_k (canopy kinetic fractionation, following Farquhar and Lloyd, 1993)	s	1.0075
δ_c (CO_2 isotopic composition at the water exchange sites in leaves)	s	50.9 ‰
$\alpha_{H2O \rightarrow CO2}$ (equilibrium fractionation factor in the canopy, following Brenninkmeijer et al., 1983)	s	1.0396
δ_e (isotopic composition of the water exchange sites in leaves)	s	11.3 ‰
δ_R (soil respiration composition, following Lee et al., 2009)	s	29.1 ±0.2 ‰
$\alpha_{k,s}$ (kinetic fractionation associated with soil respiration, following Lee et al., 2009)	sa	1.0087
δ_{soil}^{CO2} (isotopic composition of CO_2 in equilibrium with liquid water in the topsoil)	s	38.3 ±0.2 ‰
$\alpha_{H2O \rightarrow CO2}$ (equilibrium fractionation factor in the topsoil, following Brenninkmeijer et al., 1983)	s	1.0408
δ_{soil}^{liq} (isotopic composition of liquid water in topsoil (0-10 cm) samples)	m	-2.5 ±0.2 ‰

https://doi.org/10.5194/egusphere-2025-5969
Preprint. Discussion started: 18 December 2025

Author contributions. The Utrecht and Wageningen teams realized the measurement setup and contributed to the interpretation of the measurements. R.P.J. Moonen was responsible for the data analysis and writing the manuscript. G.A. Adnew was responsible for the discrete atmospheric samples. Corrections and suggestions for the manuscript were made by all authors.

Competing interests. The authors declare no conflicts of interest.

595 *Acknowledgements.* The CloudRoots project was funded by the Dutch National Science Foundation NWO (grant number OCENW.KLEIN.407). The isotope instruments used in this study were funded as part of the Ruisdael Observatory, the Dutch national atmospheric research infrastructure project which is (partly) financed by the Dutch Research Council (NWO, grant number 184.034.015). We thank Marcel Portanger (Utrecht University), Oscar Hartogensis, and Henk Snellen (Wageningen University) for their highly valuable technical support, Valmir Ferreira de Lima, Davi Silva, and Karl Kübler for their on site support at the ATTO site, Uwe Kuhn for his efforts in realising the 54 m balcony
600 at ATTO, and the entire leaf and soil sample team; Jardison Valente Nunes, Maria Juliana de Melo Monte, Gloria Vieira Rodrigues, Amanda Rayane Damasceno Macambira, and Heike Geilmann.

The ATTO project has been funded by the German Bundesministerium für Bildung und Forschung (BMBF Contracts 01LB1001A, 01LK1602B, and 01LK2101B), the Brazilian Ministério da Ciência, Tecnologia e Inovação (MCTI/FINEP Contract 01.11.01248.00), and the Max Planck Society. We also acknowledge the technical, logistic, and scientific support of the ATTO project by the Instituto Nacional de
605 Pesquisas da Amazônia (INPA), the Amazon State University (UEA), the Large-Scale Biosphere–Atmosphere Experiment (LBA), FAPEAM, the Reserva de Desenvolvimento Sustentável do Uatumã (SDS/CEUC/RDS-Uatumã), and the Max Planck Society.

https://doi.org/10.5194/egusphere-2025-5969
Preprint. Discussion started: 18 December 2025

References

Adnew, G. A., Pons, T. L., Koren, G., Peters, W., and Röckmann, T.: Leaf-scale quantification of the effect of photosynthetic gas exchange on δ17O of atmospheric CO2, Biogeosciences, 17, 3903–3922, https://doi.org/10.5194/bg-17-3903-2020, 2020.

Adnew, G. A., Hofmann, M. E., Pons, T. L., Koren, G., Ziegler, M., Lourens, L. J., and Röckmann, T.: Leaf scale quantification of the effect of photosynthetic gas exchange on Δ47 of CO2, Scientific Reports, 11, https://doi.org/10.1038/s41598-021-93092-0, 2021.

Artaxo, P.: Amazon deforestation implications in local/regional climate change, Proceedings of the National Academy of Sciences of the United States of America, 120, https://doi.org/10.1073/pnas.2317456120, 2023.

Baldocchi, D.: Measuring fluxes of trace gases and energy between ecosystems and the atmosphere - the state and future of the eddy covariance method, Global Change Biology, 20, 3600–3609, https://doi.org/10.1111/gcb.12649, 2014.

Barbour, M. M. and Farquhar, G. D.: Do pathways of water movement and leaf anatomical dimensions allow development of gradients in H218O between veins and the sites of evaporation within leaves?, Plant, Cell and Environment, 27, 107–121, https://doi.org/10.1046/j.0016-8025.2003.01132.x, 2004.

Barbour, M. M., Farquhar, G. D., and Buckley, T. N.: Leaf water stable isotopes and water transport outside the xylem, https://doi.org/10.1111/pce.12845, 2017.

Bastos, A., O'Sullivan, M., Ciais, P., Makowski, D., Sitch, S., Friedlingstein, P., Chevallier, F., Rödenbeck, C., Pongratz, J., Luijkx, I. T., Patra, P. K., Peylin, P., Canadell, J. G., Lauerwald, R., Li, W., Smith, N. E., Peters, W., Goll, D. S., Jain, A. K., Kato, E., Lienert, S., Lombardozzi, D. L., Haverd, V., Nabel, J. E., Poulter, B., Tian, H., Walker, A. P., and Zaehle, S.: Sources of Uncertainty in Regional and Global Terrestrial CO2 Exchange Estimates, Global Biogeochemical Cycles, 34, https://doi.org/10.1029/2019GB006393, 2020.

Belk, E. L., Markewitz, D., Rasmussen, T. C., Carvalho, E. J., Nepstad, D. C., and Davidson, E. A.: Modeling the effects of throughfall reduction on soil water content in a Brazilian Oxisol under a moist tropical forest, Water Resources Research, 43, https://doi.org/10.1029/2006WR005493, 2007.

Bird, R. B.: Transport phenomena, Applied Mechanics Reviews, 55, R1–R4, 2002.

Bonan, G. B.: Leaf energy fluxes (chapter 16), in: Ecological Climatology, chap. 16, pp. 229–236, Cambridge University Press, Boulder, Colorado, 2 edn., https://doi.org/https://doi.org/10.1017/CBO9780511805530.017, 2002.

Botía, S., Gerbig, C., Marshall, J., Lavric, J. V., Walter, D., Pöhlker, C., Holanda, B., Fisch, G., Carioca De Araújo, A., Sá, M. O., Teixeira, P. R., Resende, A. F., DIas-Junior, C. Q., Van Asperen, H., Oliveira, P. S., Stefanello, M., and Acevedo, O. C.: Understanding nighttime methane signals at the Amazon Tall Tower Observatory (ATTO), Atmospheric Chemistry and Physics, 20, 6583–6606, https://doi.org/10.5194/acp-20-6583-2020, 2020.

Bowling, D. R., Tans, P. P., and Monson, R. K.: Partitioning net ecosystem carbon exchange with isotopic fluxes of CO2, Global Change Biology, 7, 127–145, https://doi.org/10.1046/j.1365-2486.2001.00400.x, 2001.

Brenninkmeijer, C. A., Kraft, P., and Mook, W. G.: Oxygen isotope fractionation between CO2 and H2O, Chemical Geology, 41, 181–190, https://doi.org/10.1016/S0009-2541(83)80015-1, 1983.

Brienen, R. J., Phillips, O. L., Feldpausch, T. R., Gloor, E., Baker, T. R., Lloyd, J., Lopez-Gonzalez, G., Monteagudo-Mendoza, A., Malhi, Y., Lewis, S. L., Vásquez Martinez, R., Alexiades, M., Álvarez Dávila, E., Alvarez-Loayza, P., Andrade, A., Aragaõ, L. E., Araujo-Murakami, A., Arets, E. J., Arroyo, L., Aymard C., G. A., Bánki, O. S., Baraloto, C., Barroso, J., Bonal, D., Boot, R. G., Camargo, J. L., Castilho, C. V., Chama, V., Chao, K. J., Chave, J., Comiskey, J. A., Cornejo Valverde, F., Da Costa, L., De Oliveira, E. A., Di Fiore, A., Erwin, T. L., Fauset, S., Forsthofer, M., Galbraith, D. R., Grahame, E. S., Groot, N., Hérault, B., Higuchi, N., Honorio Coronado, E. N., Keeling,

https://doi.org/10.5194/egusphere-2025-5969
Preprint. Discussion started: 18 December 2025

H., Killeen, T. J., Laurance, W. F., Laurance, S., Licona, J., Magnussen, W. E., Marimon, B. S., Marimon-Junior, B. H., Mendoza, C., Neill, D. A., Nogueira, E. M., Núñez, P., Pallqui Camacho, N. C., Parada, A., Pardo-Molina, G., Peacock, J., Penã-Claros, M., Pickavance, G. C., Pitman, N. C., Poorter, L., Prieto, A., Quesada, C. A., Ramírez, F., Ramírez-Angulo, H., Restrepo, Z., Roopsind, A., Rudas, A., Salomaõ, R. P., Schwarz, M., Silva, N., Silva-Espejo, J. E., Silveira, M., Stropp, J., Talbot, J., Ter Steege, H., Teran-Aguilar, J., Terborgh, J., Thomas-Caesar, R., Toledo, M., Torello-Raventos, M., Umetsu, R. K., Van Der Heijden, G. M., Van Der Hout, P., Guimarães Vieira, I. C., Vieira, S. A., Vilanova, E., Vos, V. A., and Zagt, R. J.: Long-term decline of the Amazon carbon sink, Nature, 519, 344–348, https://doi.org/10.1038/nature14283, 2015.

Canet-Martí, A., Morales-Santos, A., Nolz, R., Langergraber, G., and Stumpp, C.: Quantification of water fluxes and soil water balance in agricultural fields under different tillage and irrigation systems using water stable isotopes, Soil and Tillage Research, 231, https://doi.org/10.1016/j.still.2023.105732, 2023.

Cappa, C. D., Hendricks, M. B., DePaolo, D. J., and Cohen, R. C.: Isotopic fractionation of water during evaporation, Journal of Geophysical Research: Atmospheres, 108, https://doi.org/10.1029/2003jd003597, 2003.

Cernusak, L. A., Barbour, M. M., Arndt, S. K., Cheesman, A. W., English, N. B., Feild, T. S., Helliker, B. R., Holloway-Phillips, M. M., Holtum, J. A., Kahmen, A., Mcinerney, F. A., Munksgaard, N. C., Simonin, K. A., Song, X., Stuart-Williams, H., West, J. B., and Farquhar, G. D.: Stable isotopes in leaf water of terrestrial plants, Plant Cell and Environment, 39, 1087–1102, https://doi.org/10.1111/pce.12703, 2016.

Cernusak, L. A., Wong, S. C., Stuart-Williams, H., Márquez, D. A., Pontarin, N., and Farquhar, G. D.: Unsaturation in the air spaces of leaves and its implications, https://doi.org/10.1111/pce.15001, 2024.

Craig, H. and Gordon, L. I.: Stable Isotopes in Oceanographic Studies, Tech. rep., Department of Earth Sciences and Scripps Institution of Oceanography, La Jolla, 1965.

de Deurwaerder, H. P., Visser, M. D., Detto, M., Boeckx, P., Meunier, F., Kuehnhammer, K., Magh, R. K., Marshall, J. D., Wang, L., Zhao, L., and Verbeeck, H.: Causes and consequences of pronounced variation in the isotope composition of plant xylem water, Biogeosciences, 17, 4853–4870, https://doi.org/10.5194/bg-17-4853-2020, 2020.

de Feiter, V. S., Janssens, M., de Haas, S. E., Hartogensis, O. K., Dias-Junior, C. Q., van Asperen, H., Martins, G., Miller, J. B., and Vilà-Guerau de Arellano, J.: Turbulent Exchange of CO2in the Lower Tropical Troposphere Across Clear-to-Cloudy Conditions, Journal of Geophysical Research: Atmospheres, 130, https://doi.org/10.1029/2025JD044231, 2025.

Dominguez, F., Eiras-Barca, J., Yang, Z., Bock, D., Nieto, R., and Gimeno, L.: Amazonian Moisture Recycling Revisited Using WRF With Water Vapor Tracers, Journal of Geophysical Research: Atmospheres, 127, https://doi.org/10.1029/2021JD035259, 2022.

Dongmann, G., Nürnberg, H. W., Förstel, H., and Wagener, K.: On the Enrichment of H2180 in the Leaves of Transpiring Plants, Radiation and Environmental Biophysics, pp. 41–52, 1974.

Dupont, S., Irvine, M. R., and Bidot, C.: Morning Transition of the Coupled Vegetation Canopy and Atmospheric Boundary Layer Turbulence according to the Wind Intensity, Journal of the Atmospheric Sciences, 81, 1225–1249, https://doi.org/https://doi.org/10.1175/JAS-D-23-0201.1, 2024.

Espinoza, J. C., Jimenez, J. C., Marengo, J. A., Schongart, J., Ronchail, J., Lavado-Casimiro, W., and Ribeiro, J. V. M.: The new record of drought and warmth in the Amazon in 2023 related to regional and global climatic features, Nature, Scientific Reports, 14, https://doi.org/10.1038/s41598-024-58782-5, 2024.

Farquhar, G. D. and Cernusak, L. A.: On the isotopic composition of leaf water in the non-steady state, Functional Plant Biology, 32, 293–303, https://doi.org/10.1071/FP04232, 2005.

https://doi.org/10.5194/egusphere-2025-5969
Preprint. Discussion started: 18 December 2025

Farquhar, G. D. and Gan, K. S.: On the progressive enrichment of the oxygen isotopic composition of water along a leaf, Plant, Cell and Environment, 26, 801–819, https://doi.org/10.1046/j.0016-8025.2001.00829.x-i1, 2003.

Farquhar, G. D. and Lloyd, J.: Carbon and Oxygen Isotope Effects in the Exchange of Carbon Dioxide between Terrestrial Plants and the Atmosphere, in: Stable Isotopes and Plant Carbon-water Relations, chap. 5, pp. 47–70, Academic Press, San Diego, https://doi.org/10.1016/b978-0-08-091801-3.50011-8, 1993.

Farquhar, G. D., Erleringer, J. R., and Hubick, K. T.: Carbon Isotope Discrimination and Photosynthesis, Plant Physiology, 40, 503–537, 1989a.

Farquhar, G. D., Hubick, K. T., Condon, A. G., and Richards, R. A.: Carbon Isotope Fractionation and Plant Water-Use Efficiency, in: Stable isotopes in ecological research, pp. 21–40, Springer New York, New York, 1989b.

Farquhar, G. D., Lloyd, J., Taylor, J. A., Flanagan, L. B., Syvertsen, J. P., Hubick, K. T., Wong, S. C., and Ehleringer, J. R.: Vegetation effects on the isotope composition of oxygen in atmospheric CO2, Nature, 363, 439–443, 1993.

Farquhar, G. D., Cernusak, L. A., and Barnes, B.: Heavy water fractionation during transpiration, https://doi.org/10.1104/pp.106.093278, 2007.

Finkenbiner, C. E., Li, B., Spencer, L., Butler, Z., Haagsma, M., Fiorella, R. P., Allen, S. T., Anderegg, W., Still, C. J., Noone, D., Bowen, G. J., and Good, S. P.: The NEON Daily Isotopic Composition of Environmental Exchanges Dataset, Scientific Data, 9, https://doi.org/10.1038/s41597-022-01412-4, 2022.

Fratini, G. and Mauder, M.: Towards a consistent eddy-covariance processing: An intercomparison of EddyPro and TK3, Atmospheric Measurement Techniques, 7, 2273–2281, https://doi.org/10.5194/amt-7-2273-2014, 2014.

Gentine, P., Massmann, A., Lintner, B. R., Hamed Alemohammad, S., Fu, R., Green, J. K., Kennedy, D., and Vilà-Guerau De Arellano, J.: Land-atmosphere interactions in the tropics - A review, Hydrology and Earth System Sciences, 23, 4171–4197, https://doi.org/10.5194/hess-23-4171-2019, 2019.

Gillon, J. and Yakir, D.: Influence of Carbonic Anhydrase Activity in Terrestrial Vegetation on the 18O Content of Atmospheric CO2, Tech. Rep. 5513, 2001.

González-Armas, R., Vilà-Guerau De Arellano, J., Mangan, M. R., Hartogensis, O., and De Boer, H.: Impact of canopy environmental variables on the diurnal dynamics of water and carbon dioxide exchange at leaf and canopy level, Biogeosciences, 21, 2425–2445, https://doi.org/10.5194/bg-21-2425-2024, 2024.

González-Armas, R., Rikkers, D., Hartogensis, O., Dias-Júnior, C. Q., Komiya, S., Pugliese, G., Williams, J., van Asperen, H., Vilà-Guerau de Arellano, J., and de Boer, H. J.: Daytime water and CO2 exchange within and above the Amazon rainforest, Agricultural and Forest Meteorology, 372, https://doi.org/10.1016/j.agrformet.2025.110621, 2025.

Graven, H., Keeling, R. F., and Rogelj, J.: Changes to Carbon Isotopes in Atmospheric CO2 Over the Industrial Era and Into the Future, Global Biogeochemical Cycles, 34, https://doi.org/10.1029/2019GB006170, 2020.

Griffis, T. J.: Tracing the flow of carbon dioxide and water vapor between the biosphere and atmosphere: A review of optical isotope techniques and their application, Agricultural and Forest Meteorology, 174-175, 85–109, https://doi.org/10.1016/j.agrformet.2013.02.009, 2013.

Griffis, T. J., Baker, J. M., Sargent, S. D., Tanner, B. D., and Zhang, J.: Measuring field-scale isotopic CO2 fluxes with tunable diode laser absorption spectroscopy and micrometeorological techniques, Agricultural and Forest Meteorology, 124, 15–29, https://doi.org/10.1016/j.agrformet.2004.01.009, 2004.

https://doi.org/10.5194/egusphere-2025-5969
Preprint. Discussion started: 18 December 2025

Griffis, T. J., Zhang, J., Baker, J. M., Kljun, N., and Billmark, K.: Determining carbon isotope signatures from micrometeorological measurements: Implications for studying biosphere-atmosphere exchange processes, Boundary-Layer Meteorology, 123, 295–316, https://doi.org/10.1007/s10546-006-9143-8, 2007.

Griffis, T. J., Sargent, S. D., Lee, X., Baker, J. M., Greene, J., Erickson, M., Zhang, X., Billmark, K., Schultz, N., Xiao, W., and Hu, N.: Determining the Oxygen Isotope Composition of Evapotranspiration Using Eddy Covariance, Boundary-Layer Meteorology, 137, 307–326, https://doi.org/10.1007/s10546-010-9529-5, 2010.

Hashimoto, S., Tanaka, N., Suzuki, M., Inoue, A., Takizawa, H., Kosaka, I., Tanaka, K., Tantasirin, C., and Tangtham, N.: Soil respiration and soil CO2 concentration in a tropical forest, Thailand, Journal of Forest Research, 9, 75–79, https://doi.org/10.1007/s10310-003-0046-y, 2004.

Horita, J. and Wesolowski, D. J.: Liquid-vapor fractionation of oxygen and hydrogen isotopes of water from the freezing to the critical temperature, Geochimica et Cosmochimica Acta, 58, 3425–3437, https://doi.org/10.1016/0016-7037(94)90096-5, 1994.

Jones, S. P., Kaisermann, A., Ogée, J., Wohl, S., Cheesman, A. W., Cernusak, L. A., and Wingate, L.: Oxygen isotope exchange between water and carbon dioxide in soils is controlled by pH, nitrate and microbial biomass through links to carbonic anhydrase activity, SOIL, 7, 145–159, https://doi.org/10.5194/soil-7-145-2021, 2021.

Ke, P., Ciais, P., Sitch, S., Li, W., Bastos, A., Liu, Z., Xu, Y., Gui, X., Bian, J., Goll, D. S., Xi, Y., Li, W., O'Sullivan, M., De Souza, J. G., Friedlingstein, P., and Chevallier, F.: Low latency carbon budget analysis reveals a large decline of the land carbon sink in 2023, National Science Review, 11, https://doi.org/10.1093/nsr/nwae367, 2024.

Keeling, C. D.: The concentration and isotopic abundances of atmospheric carbon dioxide in rural areas, Geochimica et Cosmochimica Acta, 13, 322–334, 1958.

Kiemle, S., Heck, K., Coltman, E., and Helmig, R.: Stable Water Isotopologue Fractionation During Soil-Water Evaporation: Analysis Using a Coupled Soil-Atmosphere Model, Water Resources Research, 59, https://doi.org/10.1029/2022WR032385, 2023.

Kolmogorov, A.: The local structure of turbulence in incompressible viscous fluid for very large Reynolds numbers, Cr. Acad. Sci. URSS, 30, 301–305, 1941.

Lee, X., Griffis, T. J., Baker, J. M., Billmark, K. A., Kim, K., and Welp, L. R.: Canopy-scale kinetic fractionation of atmospheric carbon dioxide and water vapor isotopes, Global Biogeochemical Cycles, 23, 1–15, https://doi.org/10.1029/2008GB003331, 2009.

Lee, X., Huang, J., and Patton, E. G.: A Large-Eddy Simulation Study of Water Vapour and Carbon Dioxide Isotopes in the Atmospheric Boundary Layer, Boundary-Layer Meteorology, 145, 229–248, https://doi.org/10.1007/s10546-011-9631-3, 2012.

Malhi, Y., Pegoraro, E., Nobre, A. D., Pereira, M. G., Grace, J., Culf, A. D., and Clement, R.: Energy and water dynamics of a central Amazonian rain forest, Journal of Geophysical Research: Atmospheres, 107, 45–1, https://doi.org/10.1029/2001JD000623, 2002.

Mangan, M. R., Hartogensis, O., Boone, A., Branch, O., Canut, G., Cuxart, J., de Boer, H. J., Le Page, M., Martínez-Villagrasa, D., Miró, J. R., Price, J., and Vilà-Guerau de Arellano, J.: The surface-boundary layer connection across spatial scales of irrigation-driven thermal heterogeneity: An integrated data and modeling study of the LIAISE field campaign, Agricultural and Forest Meteorology, 335, 109 452, https://doi.org/10.1016/j.agrformet.2023.109452, 2023.

Mataveli, G., Jones, M. W., Carmenta, R., Sanchez, A., Dutra, D. J., Chaves, M., de Oliveira, G., Anderson, L. O., and Aragão, L. E.: Deforestation falls but rise of wildfires continues degrading Brazilian Amazon forests, https://doi.org/10.1111/gcb.17202, 2024.

Miller, J. B. and Tans, P. P.: Calculating isotopic fractionation from atmospheric measurements at various scales, Tellus B: Chemical and Physical Meteorology, 55, 207–214, 2003.

Mook, W. G. and Geyh, M.: Environmental isotopes in the hydrological cycle, vol. 1, UNESCO, Paris, 2000.

https://doi.org/10.5194/egusphere-2025-5969
Preprint. Discussion started: 18 December 2025

Moonen, R. P. J., Adnew, G. A., Hartogensis, O. K., Vilà-Guerau De Arellano, J., Bonell Fontas, D. J., and Röckmann, T.: Data treatment and corrections for estimating H 2 O and CO 2 isotope fluxes from high-frequency observations, Atmos. Meas. Tech, 16, 5787–5810, https://doi.org/10.5194/amt-16-5787-2023, 2023.

Moonen, R. P. J., Adnew, G. A., Vilà-Guerau de Arellano, J., Hartogensis, O. K., Bonell Fontas, D. J., Komiya, S., Jones, S. P., and Röckmann, T.: Amazon rainforest ecosystem exchange of CO2 and H2O through turbulent understory ejections, Atmospheric Chemistry and Physics, 25, 12 197–12 212, https://doi.org/10.5194/acp-25-12197-2025, 2025.

Moreira, D. M., Papa, F., Fassoni-Andrade, A., Fleischmann, A. S., Wongchuig, S., Paiva, R. C. D. d., Paris, A., Frappart, F., Melo, J. S., Crétaux, J.-F., Santos, A. L. M. R. d., Garambois, P.-A., Kitambo, B., and Calmant, S.: Widespread and Exceptional Reduction in River Water Levels Across the Amazon Basin during the 2023 Extreme Drought Revealed by Satellite Altimetry and SWOT, Geophysical Research Letters, Preprint, https://doi.org/10.22541/essoar.172408211.17914763/v1, 2024.

Nocentini, A., Supuran, C. T., and Capasso, C.: An overview on the recently discovered iota-carbonic anhydrases, https://doi.org/10.1080/14756366.2021.1972995, 2021.

Oikawa, P. Y., Sturtevant, C., Knox, S. H., Verfaillie, J., Huang, Y. W., and Baldocchi, D. D.: Revisiting the partitioning of net ecosystem exchange of CO2 into photosynthesis and respiration with simultaneous flux measurements of 13CO2 and CO2, soil respiration and a biophysical model, CANVEG, Agricultural and Forest Meteorology, 234-235, 149–163, https://doi.org/10.1016/j.agrformet.2016.12.016, 2017.

Pedruzo-Bagazgoitia, X., Patton, E. G., Moene, A. F., Ouwersloot, H. G., Gerken, T., Machado, L. A., Martin, S. T., Sörgel, M., Stoy, P. C., Yamasoe, M. A., and Vilà-Guerau de Arellano, J.: Investigating the Diurnal Radiative, Turbulent, and Biophysical Processes in the Amazonian Canopy-Atmosphere Interface by Combining LES Simulations and Observations, Journal of Advances in Modeling Earth Systems, 15, https://doi.org/10.1029/2022MS003210, 2023.

Ronda, R. J., De Bruin, H. A. R., and Holtslag, A. A. M.: Representation of the canopy conductance in modeling the surface energy budget for low vegetation, Journal of Applied Meteorology, 40, 1431–1444, 2001.

Rothfuss, Y. and Javaux, M.: Reviews and syntheses: Isotopic approaches to quantify root water uptake: A review and comparison of methods, Biogeosciences, 14, 2199–2224, https://doi.org/10.5194/bg-14-2199-2017, 2017.

Sabot, M. E., De Kauwe, M. G., Pitman, A. J., Medlyn, B. E., Ellsworth, D. S., Martin-StPaul, N. K., Wu, J., Choat, B., Limousin, J. M., Mitchell, P. J., Rogers, A., and Serbin, S. P.: One Stomatal Model to Rule Them All? Toward Improved Representation of Carbon and Water Exchange in Global Models, Journal of Advances in Modeling Earth Systems, 14, https://doi.org/10.1029/2021MS002761, 2022.

Schellekens, J., Bruijnzeel, L. A., Scatena, F. N., Bink, N. J., and Holwerda, F.: Evaporation from a tropical rain forest, Luquillo Experimental Forest, eastern Puerto Rico, Water Resources Research, 36, 2183–2196, https://doi.org/10.1029/2000WR900074, 2000.

Spiridonov, V. and Ćurić, M.: Atmospheric Boundary Layer (ABL), in: Fundamentals of Meteorology, chap. 14, pp. 219–228, Springer International Publishing, Cham, https://doi.org/10.1007/978-3-030-52655-9_14, 2021.

Stoy, P. C., El-Madany, T. S., Fisher, J. B., Gentine, P., Gerken, T., Good, S. P., Klosterhalfen, A., Liu, S., Miralles, D. G., Perez-Priego, O., Rigden, A. J., Skaggs, T. H., Wohlfahrt, G., Anderson, R. G., Coenders-Gerrits, A. M. J., Jung, M., Maes, W. H., Mammarella, I., Mauder, M., Migliavacca, M., Nelson, J. A., Poyatos, R., Reichstein, M., Scott, R. L., and Wolf, S.: Reviews and syntheses: Turning the challenges of partitioning ecosystem evaporation and transpiration into opportunities, Biogeosciences, 16, 3747–3775, https://doi.org/10.5194/bg-16-3747-2019, 2019.

https://doi.org/10.5194/egusphere-2025-5969
Preprint. Discussion started: 18 December 2025

Sutanto, S. J., Van Den Hurk, B., Dirmeyer, P. A., Seneviratne, S. I., Röckmann, T., Trenberth, K. E., Blyth, E. M., Wenninger, J., and Hoffmann, G.: HESS Opinions "a perspective on isotope versus non-isotope approaches to determine the contribution of transpiration to total evaporation", Hydrology and Earth System Sciences, 18, 2815–2827, https://doi.org/10.5194/hess-18-2815-2014, 2014.

Tans, P. P.: Oxygen isotopic equilibrium between carbon dioxide and water in soils, Tellus B, 50, 163–178, https://doi.org/10.1034/j.1600-0889.1998.t01-1-00004.x, 1998.

Tramontana, G., Migliavacca, M., Jung, M., Reichstein, M., Keenan, T. F., Camps-Valls, G., Ogee, J., Verrelst, J., and Papale, D.: Partitioning net carbon dioxide fluxes into photosynthesis and respiration using neural networks, Global Change Biology, 26, 5235–5253, https://doi.org/10.1111/gcb.15203, 2020.

van der Velde, I. R., Miller, J. B., Schaefer, K., Van Der Werf, G. R., Krol, M. C., and Peters, W.: Terrestrial cycling of 13CO2 by photosynthesis, respiration, and biomass burning in SiBCASA, Biogeosciences, 11, 6553–6571, https://doi.org/10.5194/bg-11-6553-2014, 2014.

Vilà-Guerau de Arellano, J., Hartogensis, O., Benedict, I., de Boer, H., Bosman, P. J. M., Botía, S., Cecchini, M. A., Faassen, K. A. P., González-Armas, R., van Diepen, K., Heusinkveld, B. G., Janssens, M., Lobos-Roco, F., Luijkx, I. T., Machado, L. A. T., Mangan, M. R., Moene, A. F., Mol, W. B., van der Molen, M., Moonen, R., Ouwersloot, H. G., Park, S., Pedruzo-Bagazgoitia, X., Röckmann, T., Adnew, G. A., Ronda, R., Sikma, M., Schulte, R., van Stratum, B. J. H., Veerman, M. A., van Zanten, M. C., and van Heerwaarden, C. C.: Advancing understanding of land–atmosphere interactions by breaking discipline and scale barriers, Annals of the New York Academy of Sciences, pp. 74–97, https://doi.org/https://doi.org/10.1111/nyas.14956, 2023.

Vilà-Guerau de Arellano, J., Hartogensis, O. K., de Boer, H., Moonen, R., González-Armas, R., Janssens, M., Adnew, G. A., Bonell-Fontás, D. J., Botía, S., Jones, S. P., van Asperen, H., Komiya, S., de Feiter, V. S., Rikkers, D., de Haas, S., Machado, L. A., Dias-Junior, C. Q., Giovanelli-Haytzmann, G., Valenti, W. I., Figueiredo, R. C., Farias, C. S., Hall, D. H., Mendonça, A. C., da Silva, F. A., Silva, J. L. d., Souza, R., Martins, G., Miller, J. N., Mol, W. B., Heusinkveld, B., van Heerwaarden, C. C., D'Oliveira, F. A., Ferreira, R. R., Gotuzzo, R. A., Pugliese, G., Williams, J., Ringsdorf, A., Edtbauer, A., Quesada, C. A., Portela, B. T. T., Alves, E. G., Pöhlker, C., Trumbore, S., Lelieveld, J., and Röckmann, T.: CloudRoots-Amazon22: Integrating Clouds with Photosynthesis by Crossing Scales, Bulletin of the American Meteorological Society, 105, E1275–E1302, https://doi.org/10.1175/BAMS-D-23-0333.1, 2024.

Wahl, S., Steen-Larsen, H. C., Reuder, J., and Hörhold, M.: Quantifying the Stable Water Isotopologue Exchange Between the Snow Surface and Lower Atmosphere by Direct Flux Measurements, Journal of Geophysical Research: Atmospheres, 126, https://doi.org/10.1029/2020JD034400, 2021.

Webb, E. K., Pearman, G. I., and Leuning, R.: Correction of flux measurements for density effects due to heat and water vapour transfer, Quarterly Journal of the Royal Meteorological Society, 106, 85–100, https://api.semanticscholar.org/CorpusID:122687161, 1980.

Wehr, R. and Saleska, S. R.: An improved isotopic method for partitioning net ecosystem-atmosphere CO2 exchange, Agricultural and Forest Meteorology, 214-215, 515–531, https://doi.org/10.1016/j.agrformet.2015.09.009, 2015.

Wei, Z., Yoshimura, K., Wang, L., Miralles, D. G., Jasechko, S., and Lee, X.: Revisiting the contribution of transpiration to global terrestrial evapotranspiration, Geophysical Research Letters, 44, 2792–2801, https://doi.org/10.1002/2016GL072235, 2017.

Wilczak, J. M., Oncley, S. P., and Stage, S. A.: Sonic anemometer tilt correction algorithms, Boundary-Layer Meteorology, 99, 127–150, 2001.

Wingate, L., Ogée, J., Cuntz, M., Genty, B., Reiter, I., Seibt, U., Yakir, D., Maseyk, K., Pendall, E. G., Barbouri, M. M., Mortazavij, B., Burlett, R., Peylin, P., Miller, J., Mencuccini, M., Shim, J. H., Hunt, J., and Grace, J.: The impact of soil microorganisms on the global

https://doi.org/10.5194/egusphere-2025-5969
Preprint. Discussion started: 18 December 2025

budget of δ18O in atmospheric CO2, Proceedings of the National Academy of Sciences of the United States of America, 106, 22 411–22 415, https://doi.org/10.1073/pnas.0905210106, 2009.

Yakir, D. and da Silveira Lobo Sternberg, L.: The use of stable isotopes to study ecosystem gas exchange, Oecologia, 123, 297–311, 2000.

York, D.: Least squares fitting of a straight line with correlated errors, Earth and Planetary Science Letters, 5, 320–324, https://doi.org/10.1016/S0012-821X(68)80059-7, 1968.

Zhiña, D. X., Mosquera, G. M., Esquivel-Hernández, G., Córdova, M., Sánchez-Murillo, R., Orellana-Alvear, J., and Crespo, P.: Hydrometeorological factors controlling the stable isotopic composition of precipitation in the highlands of south Ecuador, Journal of Hydrometeorology, 23, 1059–1074, 2022.